

Forecasting COVID-19 Pandemic: A Data-Driven Analysis

Khondoker Nazmoon Nabi (✉ nabinil@yahoo.com)

Bangladesh University of Engineering and Technology (BUET) <https://orcid.org/0000-0003-2337-0226>

Research Article

Keywords: Compartmental model, COVID-19, coronavirus, asymptomatic carrier, quarantined class, model calibration, sensitivity

Posted Date: May 21st, 2020

DOI: <https://doi.org/10.21203/rs.3.rs-30396/v1>

License:  This work is licensed under a Creative Commons Attribution 4.0 International License.

[Read Full License](#)

Version of Record: A version of this preprint was published at Chaos, Solitons & Fractals on October 1st, 2020. See the published version at <https://doi.org/10.1016/j.chaos.2020.110046>.

FORECASTING COVID-19 PANDEMIC: A DATA-DRIVEN ANALYSIS

Khondoker Nazmoon Nabi

Department of Mathematics, Bangladesh University of Engineering and Technology (BUET), Dhaka-1000, Bangladesh.

Abstract

In this paper, a new Susceptible-Exposed-Symptomatic Infectious-Asymptomatic Infectious-Quarantined-Hospitalized-Recovered-Dead ($SEI_D I_U QHRD$) deterministic compartmental model has been proposed and calibrated for interpreting the transmission dynamics of the novel coronavirus disease (COVID-19). The purpose of this study is to give a tentative prediction of the epidemic peak for Russia, Brazil, India and Bangladesh which could become the next COVID-19 hotspots in no time by using a Trust-region-reflective (TRR) algorithm which one of the well-known real data fitting techniques. Based on the publicly available epidemiological data from late January until 10 May, it has been estimated that the number of daily new symptomatic infectious cases for the above mentioned countries could reach the peak around the beginning of June with the peak size of $\sim 15,774$ (95% CI, 13,814-17,734) symptomatic infectious cases in Russia, $\sim 26,449$ (95% CI, 23,489-29,409) cases in Brazil, $\sim 9,504$ (95% CI, 8,378-10,630) cases in India and $\sim 2,209$ (95% CI, 1,878-2,540) cases in Bangladesh. As of May 11, 2020, incorporating the infectiousness capability of asymptomatic carriers, our analysis estimates the value of the basic reproduction number (R_0) as of May 11, 2020 was found to be ~ 4.234 (95% CI, 3.764-4.7) in Russia, ~ 5.347 (95% CI, 4.737-5.95) in Brazil, ~ 5.218 (95% CI, 4.56-5.81) in India, ~ 4.649 (95% CI, 4.17-5.12) in the United Kingdom and ~ 3.53 (95% CI, 3.12-3.94) in Bangladesh. Moreover, Latin hypercube sampling-partial rank correlation coefficient (LHS-PRCC) which is a global sensitivity analysis (GSA) method is applied to quantify the uncertainty of our model mechanisms, which elucidates that for Russia, the recovery rate of undetected asymptomatic carriers, the rate of getting home-quarantined or self-quarantined and the transition rate from quarantined class to susceptible class are the most influential parameters, whereas the rate of getting home-quarantined or self-quarantined and the inverse of the COVID-19 incubation period are highly sensitive parameters in Brazil, India, Bangladesh and the United Kingdom which could significantly affect the transmission dynamics of the novel coronavirus. Our analysis also suggests that relaxing social distancing restrictions too quickly could exacerbate the epidemic outbreak in the above-mentioned countries.

Keywords: Compartmental model, COVID-19, coronavirus, asymptomatic carrier, quarantined class, model calibration, sensitivity.

Email address: nabinil@yahoo.com (Khondoker Nazmoon Nabi)

1. Introduction

The coronavirus disease 2019 (COVID-19) has evolved as a global public health emergency affecting 212 countries and territories around the world as of May 12, 2020 [Worldometer, \(2020\)](#). COVID-19 is one kind of respiratory disease by the novel coronavirus (SARS-CoV-2) that was first spotted around late December 2019, in Wuhan, Hubei province, China [Li et al., \(2020\)](#); [Zhou et al., \(2020\)](#). This novel virus started transmitting around the world rapidly, and on 30 January, WHO declared the outbreak as a Public Health Emergency of International Concern (PHEIC). Later, WHO Director-General announced COVID-19 as a global pandemic. As of May 11, 2020, an outbreak of COVID-19 has resulted in 4,271,689 confirmed cumulative cases with reported deaths of 287,613 worldwide [Worldometer, \(2020\)](#). In most of the countries, infected patients are struggling to get the proper treatment due to highly transmissible and virulent nature of the virus. Nevertheless, numerous COVID-19 mitigation strategies has been adapted so far such as quarantine, isolation, promoting the wearing of face masks, travel restrictions, and lockdowns with a view to reducing community transmission of the disease.

In the absence of either established effective treatment or a vaccine, the already fragile health care systems of different developed and developing countries can be overburdened due to the overwhelming surge of infections in in the coming months provided that the spread is not controlled. This pandemic is giving an upsurge to multifarious noteworthy socio-economic and public health impacts and has highlighted the significance of detecting the evolution of the disease and prediction of disease future dynamics for designing infectious disease prevention and control strategies, effective public health policies and economical activity guidelines. Different mathematical paradigms have always played a notable role in providing deeper understanding of the transmission mechanisms of a disease outbreak, contributing considerable insights for controlling the disease outbreak. One of the familiar models for human-to-human transmission which is reasonably predictive is Susceptible-Infectious-Removed (SIR) epidemic model proposed by Kermack-Mckendrick in 1927 [Calafiore et al., \(2020\)](#); [Nesteruk \(2020\)](#). After that, the SIR epidemic model has been extended to Susceptible-Exposed-Infectious-Removed (SEIR) model and many of its variants to explore the risk factors of a disease or predict the dynamics of a disease outbreak [Wu et al., \(2020\)](#); [Calafiore et al., \(2020\)](#); [kucharski et al., \(2020\)](#); [Simha et al., \(2020\)](#); [Anastassopoulou et al., \(2020\)](#); [Nesteruk \(2020\)](#). It is really challenging in population based model to incorporate certain real-world complexities. In fact, analysis and prediction could go wrong in the absence of adequate historical real data. On the other hand, various agent-based often stochastic models where individuals interact on a network structure and get infected stochastically, have been treated as useful tools for tracing fine-grained effects of heterogeneous intervention policies in diverse disease outbreaks [Ferguson et al., \(2020\)](#); [Chang et al., \(2020\)](#); [Wilder et al., \(2020\)](#); [Ruiz et al., \(2020\)](#). However, accuracy of this approach can be a vital issue due to the time-varying nature of network-structure.

Since the outbreak of the virus, incorporating travel between major cities in China, [Li et al., \(2020\)](#) proposed an SEIR-model incorporating a metapopulation structure for both reported and unreported infections. It has been discovered in their studies that around 86% of all cases went undetected in Wuhan before travel restrictions imposed on January 23, 2020. According to their estimation, on an individual basis, around

47 55% asymptomatic spreaders were contagious who were responsible for 79% of new
48 infected cases. Other studies [Ferguson et al., \(2020\)](#); [Verity et al., \(2020\)](#) solidified
49 the significance of incorporating asymptomatic carriers with a view to understanding
50 COVID-19 future dynamics appropriately. Later, [Calafiore et al., \(2020\)](#) estimated
51 that around 63% cases went under-reported in Italy by analyzing a modified SIR-
52 model. [Anastassopoulou et al., \(2020\)](#) apply the SIRD model to Chinese official
53 statistics, estimating parameters using linear regression and predict the COVID-19
54 pandemic in Hubei province by using these models and parameters. Nonetheless, long-
55 term forecasting is debatable while using a simple mathematical model. [Diego Caccavo,](#)
56 [\(2020\)](#) and [Peter Turchin, \(2020\)](#) independently apply modified SIRD models, in which
57 parameters change overtime following specific function forms. Parameters govern these
58 functions are estimated by minimizing the sum-of-square-error. However, using the
59 sum-of-square method causes over-fitting and always favors a complex model, therefore
60 it is not suitable to assess policy effectiveness. Moreover, fitting the SIRD model in
61 the early stage of infection is questionable as well.

62 In the light of above shortcomings of several established mathematical models,
63 a more refined deterministic system of nonlinear differential equations, considering
64 all possible interactions, a Susceptible-Exposed-Symptomatic Infectious-Asymptomatic
65 Infectious-Quarantined-Hospitalized-Recovered-Dead ($SEI_D I_U QHRD$) model has been
66 proposed, which can give more accurate and robust short-term as well as long-term
67 predictions of COVID-19 future dynamics. This model could be considered as a gen-
68 eralization of SEIR, which is based on the introduction of asymptomatic infectious
69 state, quarantined state in order to understand the effect of preventive actions and
70 hospitalized (isolated) state. Based on similar studies performed over SEIR dynamical
71 systems some assumptions are taken into account [Wu et al., \(2020\)](#); [Calafiore et al.,](#)
72 [\(2020\)](#); [Anastassopoulou et al., \(2020\)](#). As of May 11, it is evident that how the early
73 stage mathematical model parameters have changed drastically as detection rate was
74 really low until middle of February, however the outbreak situation has improved com-
75 prehensively in several countries due to massive scale testing [Qianying et al. \(2020\)](#).
76 We have considered the nominal values of the model parameters understanding the
77 characteristics of the coronavirus infection, quantitatively estimated in the literature
78 or published by health organizations [Read et al., \(2020\)](#); [Li et al., \(2020\)](#); [Wu et al.,](#)
79 [\(2020\)](#); [Verity et al., \(2020\)](#). In sequence, a rigorous process of model calibration
80 which is known as Trust-region-reflective algorithm is applied to determine the best-
81 fitted parameter values of the model. Our analysis was based on the publicly available
82 data of the new confirmed daily cases reported for the future probable COVID-19
83 hotspots which are Russia, Brazil, India and Bangladesh from late January until May
84 09, 2020 [Center for Systems Science and Engineering at Johns Hopkins University,](#)
85 [\(2020\)](#). Further, we have validated our model for the United Kingdom using same
86 time frame. Based on the released data, we attempted to estimate the mean values of
87 the crucial epidemiological parameters for COVID-19, such as the infectiousness factor
88 for asymptomatic carriers, isolation period, the estimation of the inflection point with
89 probable date, recovery period for both symptomatic and asymptomatic individuals,
90 case-fatality ratio and mortality rate in those potential hotspots. Perfect data-driven
91 and curve-fitting methods for the prediction of any disease outbreak have always been
92 question of interest in epidemiological research. Trust-region-reflect algorithm is one of

93 the robust least-square data-fitting techniques that can promote a fine relation between
94 the model driving mechanisms and model responses. This real-time data fitting ap-
95 proach could be efficient providing considerable insights on disease outbreak dynamics
96 in different countries and designing worthwhile public health policies in curtailing the
97 disease burden. Calibrating our model parameters by using the above algorithm, we
98 have provided probable forecasts for the newly evolving COVID-19 hotspots.

99 This paper is organized as follows. In section 2, the mathematical model is described
100 and the background of choosing baseline parameter values for the model is discussed. In
101 section 3 and 4, the model has been analysed and model calibration technique has been
102 discussed respectively. In section 5, model prediction accuracy has been illustrated by
103 representing a graphical comparison between model responses and real-time data. In
104 section 6, one of the robust global sensitivity analysis techniques is used to quantify
105 the most influential mechanisms in our model. This paper ends with some qualitative
106 and quantitative observations and discussions.

107 2. Formulation of the Mathematical Model

108 In this work, we use a compartmental differential equation model for the spread
109 of COVID-19 in the world. The spread of the infection starts with the introduction
110 of a small group of infected individuals to a large population. In this model we focus our
111 study on eight components of the epidemic flow, i.e. $\{S(t), E(t), I_D(t), I_U(t), Q(t), H(t), R(t), D(t)\}$
112 which represent the number of the susceptible individuals, exposed individuals (infected
113 however not yet to be infectious, in an incubation period), symptomatic infectious indi-
114 viduals (confirmed with infectious capacity), asymptomatic infectious individuals (un-
115 detected but infectious), quarantined, hospitalized (under treatment), recovered cases
116 (immuned) and death cases (or closed cases). Then the entire number of population in
117 a certain region or country is $N = S + E + I_D + I_U + Q + H + R + D$. The following
118 assumptions are considered in the formulation of the model:

- 119 • Emigration from the population and immigration into the population have not
120 been taken into account in model formulation as there is negligible proportion of
121 individuals move in and out of the population at a specific time frame.
- 122 • Births and natural deaths in the population are not considered.
- 123 • The susceptible population are exposed to a latent class .
- 124 • Hospitalized patients cannot spread disease while in isolation treatment after
125 confirmed diagnosis.
- 126 • Recovered individuals do not return to susceptible class as they develop certain
127 immunity against the disease. Hence they cannot become re-infected again and
128 cannot infect susceptible either.

129 Figure 1 is the flow diagram of the proposed model, where susceptible individu-
130 als (S) get infected at a baseline infectious contact rate β , via contact with either
131 symptomatic infectious individuals (I_D) or at a rate $\beta\lambda$ of asymptomatic infectious
132 carriers and move to exposed (E) class. The relative infectiousness capacity of asymp-
133 tomatic spreaders is λ (related to symptomatic infectious individuals). Susceptible

134 individuals can be quarantined with contact tracing procedure and the rate of getting
 135 home-quarantined or self-quarantined of S is q , whereas κ is the rate of progression
 136 of symptoms of COVID-19 (hence $\frac{1}{\kappa}$ is the mean incubation period of COVID-19).
 137 Detected symptomatic infected individuals are generated at a progression rate σ_1 and
 138 undetected asymptomatic infectious cases are generated at a rate σ_2 from the exposed
 139 class. In addition, individuals who are exposed to virus can be quarantined with contact
 140 tracing procedure at a rate $(1 - \sigma_1 - \sigma_2)$. γ is the rate of confirmation and isolation after
 141 symptom onset in detected infectious individuals and $1/\gamma$ is the time period when the
 142 infection can spread. The proportion of individuals from quarantined to symptomatic
 143 infectious, asymptomatic infectious and susceptible are $r_2\eta$, $r_1\eta$ and $(1 - r_1 - r_2)\eta$
 144 respectively. δ_U is the disease-induced death rate for undetected asymptomatic pa-
 145 tients and δ_H is the death rate for hospitalized patients. ϕ_D , ϕ_U and ϕ_H are recovery
 146 rates for the symptomatic patients, asymptomatic carriers and hospitalized patients
 147 respectively. In addition, $1/\phi_D$, $1/\phi_U$ and $1/\phi_H$ represent the mean period of isolation
 148 for the detected symptomatic infectious individuals, undetected asymptomatic carriers
 and hospitalized patients. Based on these assumptions, the basic model structure for

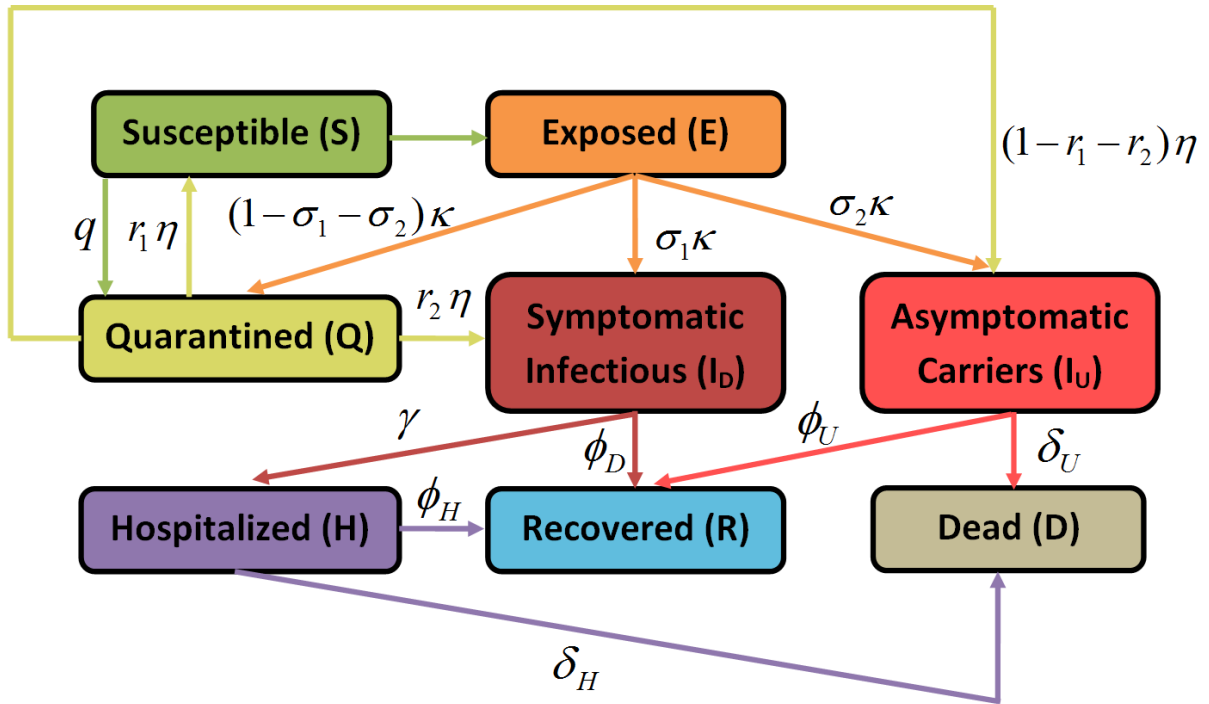


Figure 1: A schematic diagram that illustrates the proposed COVID-19 model

149 the transmission dynamics of COVID-19 is illustrated by the following deterministic
 150

151 framework of nonlinear differential equations (1).

$$\left\{ \begin{array}{l}
 \frac{dS}{dt} = -\beta S \frac{(I_D + \lambda I_U)}{N - D} + r_1 \eta Q - qS, \\
 \frac{dE}{dt} = \beta S \frac{(I_D + \lambda I_U)}{N - D} - \kappa E, \\
 \frac{dI_D}{dt} = \sigma_1 \kappa E - \gamma I_D - \phi_D I_D + r_2 \eta Q, \\
 \frac{dI_U}{dt} = \sigma_2 \kappa E - \phi_U I_U - \delta_U I_U + (1 - r_1 - r_2) \eta Q \\
 \frac{dQ}{dt} = (1 - \sigma_1 - \sigma_2) \kappa E - \eta Q + qS \\
 \frac{dH}{dt} = \gamma I_D - \phi_H H - \delta_H H \\
 \frac{dR}{dt} = \phi_D I_D + \phi_U I_U + \phi_H H \\
 \frac{dD}{dt} = \delta_U I_U + \delta_H H
 \end{array} \right. \quad (1)$$

152 2.1. Baseline epidemiological parameters

153 In the study of [Lauer et al., \(2020\)](#), the average incubation period of COVID-19
 154 was calculate to be 5.1 days and similar model-based studies also justified the above
 155 finding [Li et al., \(2020\)](#); [Ferguson et al., \(2020\)](#); [Tang et al., \(2020\)](#). Moreover, within
 156 11.5 days (i.e. $\kappa = 1/11.5 \text{ day}^{-1}$) of infection, the individuals who were exposed to the
 157 virus started developing symptoms [Lauer et al., \(2020\)](#); [Verity et al., \(2020\)](#) and 20.0
 158 days was the mean duration of viral shedding observed in COVID-19 survivors [Zhou et](#)
 159 [al., \(2020\)](#). The time duration from symptoms onset to recovery was estimated to be
 160 24.7 days, whereas from onset of symptoms to death, the average mean duration was
 161 estimated to be 17 Δ 8 days [Verity et al., \(2020\)](#). In previous modeling studies, [Shen](#)
 162 [et al. \(2020\)](#); [Read et al., \(2020\)](#); [Li et al., \(2020\)](#), the novel coronavirus effective
 163 transmission rate, β ranges from around $0.25 - 1.5 \text{ day}^{-1}$, which gradually follows a
 164 downward trend with time [Tang et al., \(2020\)](#). In sequence, we have considered this
 165 parameter as a time-varying parameter in our fits. Table 1 illustrates the list of baseline
 166 model parameters with brief description, probable ranges presented on clinical studies
 167 and calibration, and default base value selected for our study.

168 2.2. Dataset

169 The recent epidemic data of five different countries which are Russia, Brazil, India,
 170 Bangladesh and the United Kingdom is accumulated from authoritative and genuine
 171 sources which are Center of Disease Control and Prevention (CDC) and the COVID
 172 Tracking Project (testing and hospitalizations). The data repository is handled by the
 173 Johns Hopkins University Center for Systems Science and Engineering (JHU CSSE)
 174 and supported by ESRI Living Atlas Team and the Johns Hopkins University Applied
 175 Physics Lab (JHU APL). The repository is publicly available and easy to compile
 176 [Center for Systems Science and Engineering at Johns Hopkins University, \(2020\)](#).

Parameter	Definition	Units	Likely Range	Default Value	References
β	infectious contact rate	day^{-1}	0.2 – 1.5	0.5	Shen et al. (2020); Read et al., (2020); Li et al., (2020)
λ	infectiousness factor for unde- tected infected carrier	-	0.4-0.6	0.5	Li et al., (2020); Fergu- son et al., (2020)
r_1	fraction of quarantined that be- come susceptible	-	0.7-0.99	0.9	Calibrated
r_2	fraction of quarantined that be- come detected symptomatic	-	0.005-0.1	0.02	Calibrated
η	transition from quarantined to either infectious or susceptible	day^{-1}	0.005-0.3	0.01	Calibrated
κ	transition exposed to infectious	day^{-1}	$\frac{1}{14} - \frac{1}{3}$	1/5.1	Li et al., (2020); Lauer et al., (2020)
q	transition susceptible to quar- antined	day^{-1}	0.001-0.5	0.01	Calibrated
σ_1	fraction of infections that be- come detected symptomatic	-	0.0001- 0.1	0.0032	Calibrated
σ_2	fraction of infections that be- come undetected symptomatic	-	0.01-0.95	0.5	Calibrated
γ	transition detected symp- tomatic to hospitalized	day^{-1}	0.2-0.9	0.5	Ferguson et al., (2020); Zhou et al., (2020)
ϕ_D	Recovery rate, detected symp- tomatic	day^{-1}	$\frac{1}{30} - \frac{1}{3}$	1/7	Tang et al., (2020); Zhou et al., (2020)
ϕ_U	Recovery rate, undetected symptomatic	day^{-1}	$\frac{1}{30} - \frac{1}{3}$	1/7	Tang et al., (2020); Zhou et al., (2020)
ϕ_H	Recovery rate, Hospitalized	day^{-1}	$\frac{1}{30} - \frac{1}{3}$	1/7	Tang et al., (2020); Zhou et al., (2020)
δ_U	Disease induced death rate, un- detected symptomatic	day^{-1}	0.001-0.1	0.015	Ferguson et al., (2020)
δ_H	disease induced death rate, hos- pitalized	day^{-1}	0.001-0.1	0.015	Ferguson et al., (2020)

Table 1: Model parameters with brief definition and probable ranges based on model calibration, relevant literature and clinical studies

177 **3. Analysis of the Model**

178 *3.1. Disease Free Equilibrium (DFE)*

179 The disease-free equilibrium (DFE) of (1) can be obtained easily by setting $S =$
 180 $E = I_D = I_U = Q = H = R = D = 0$. Therefore the DFE of (1) is :

$$E_0 = (S_0^*, E_0^*, I_{D_0}^*, I_{U_0}^*, Q_0^*, H_0^*, R_0^*, D_0^*) = (0, 0, 0, 0, 0)$$

181 *3.2. Basic Reproduction Number for Proposed Model*

182 Using the next generation operator method [Van den Driessche et al. \(2002\)](#) the
 183 local stability of the DFE is investigated. According to the notation in [Diekmann et](#)
 184 [al., \(1990\)](#), the associated non-negative matrix, \mathcal{F} represents new infection terms, and
 185 the non-singular matrix, \mathcal{V} denotes remaining transfer terms which can be described as
 186 follows:

187

$$\mathcal{F} = \begin{pmatrix} 0 & \beta & \beta\lambda \\ 0 & 0 & 0 \\ 0 & 0 & 0 \end{pmatrix}$$

188

189 and

$$\mathcal{V} = \begin{pmatrix} k & 0 & 0 \\ -\sigma_1 k & \gamma + \phi_D & 0 \\ -\sigma_2 k & 0 & \phi_U + \delta_U \end{pmatrix}$$

190 The associated basic reproduction number, denoted by \mathcal{R}_0 is then given by,
 191 $\mathcal{R}_0 = \rho(\mathcal{F}\mathcal{V}^{-1})$, where ρ is the spectral radius of $\mathcal{F}\mathcal{V}^{-1}$. It follows that,

$$\mathcal{R}_0 = \frac{\beta [\delta_U \sigma_1 + (\gamma + \phi_D) \lambda \sigma_2 + \sigma_1 \phi_U]}{(\gamma + \phi_D) (\delta_U + \phi_U)} \quad (2)$$

192 Thus, by Theorem 2 of [LaSalle \(1976\)](#), the following result is established.

193 **Lemma 1.** *The DFE, E_0 of the system (1), is locally-asymptotically stable (LAS) if*
 194 *$\mathcal{R}_0 < 1$, and unstable if $\mathcal{R}_0 \geq 1$*

195 The threshold quantity, \mathcal{R}_0 , estimates the mean number of secondary cases gen-
 196 erated by a single infected individual in an entirely susceptible human population
 197 [Hethcote \(2000\)](#). The above result implies that a small influx of infected individuals
 198 would not generate large outbreaks if $\mathcal{R}_0 < 1$, and the disease will persist (be endemic)
 199 in the population if $\mathcal{R}_0 > 1$.

200 **4. Model Calibration**

201 The proposed epidemic model (1) is a continuous-time non-linear system of dif-
 202 ferential equations together with a suitable set of initial conditions. In this study,
 203 Trust-region-reflective (TRR) algorithm has been used to determine the best-fitted pa-
 204 rameters for our proposed model. We have used **lsqcurvefit** function in MATLAB to
 205 calibrate our model. The optimization process can be expressed as follows:

$$\theta^* = \arg \min_{\theta} := \left\| SEI_D I_U QHRD(\theta, time) - \begin{pmatrix} I_D \\ R \\ D \end{pmatrix} \right\|^2$$

206 where θ^* is the set of parameters of dynamically calibrated model, $\{I_D, R, D\}$ is a set of
 207 the detected symptomatic infectious individuals, recovered and disease induced death
 208 cases from the real-time data and $\theta = \{\beta, \lambda, r_1, r_2, \eta, k, \sigma_1, \sigma_2, \gamma, q, \phi_D, \phi_U, \phi_H, \delta_U, \delta_H\}$
 209 is the initial set of parameters of the proposed model and $SEI_D I_U QHRD(\cdot)$ represents
 210 our proposed model. The ‘‘TRR algorithm’’ also necessitates an initial guess for each
 211 parameter which is described as ‘‘TRR input’’ in the following section.

212 5. Numerical Experiments and Forecasting

213 In this section, we have used dynamically calibrated compartment model for real-
 214 time analysis and real-time prediction of COVID-19 outbreak for five different countries
 215 which are Russia, Brazil, India, Bangladesh and the United Kingdom. Figure 2, 4, 6,
 216 8, 10 illustrates the best real-time data fitting results using the baseline parameters
 217 from Table 1 as initial inputs for our proposed model. The ranges of the parameters
 218 and have been set compatible with the clinical studies and illustrated 2, 3, 4, 5, 6 along
 219 with the parameters resulted from the calibration (‘‘TRR output’’). To ensure a huge
 220 number of susceptible individuals at the initial stage of an outbreak, $0.9N$ has been
 221 set as a lower bound for S .

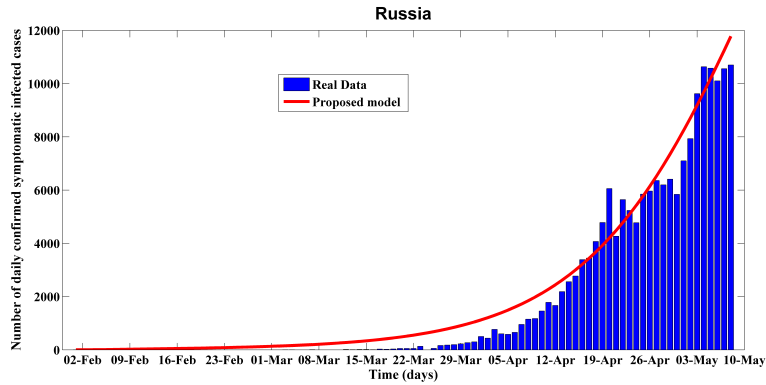
222 5.1. Analysis and prediction for Russia

223 With much of Europe now easing itself out of confinement, Russia could become
 224 the continent’s new Covid-19 hotspot according to our analysis. The model fitting and
 225 projection results for Russia from early February to late August are shown in Figure 2
 226 and 3. We collected real data from February 01 to May 08, 2020 to calibrate the model
 227 parameters.

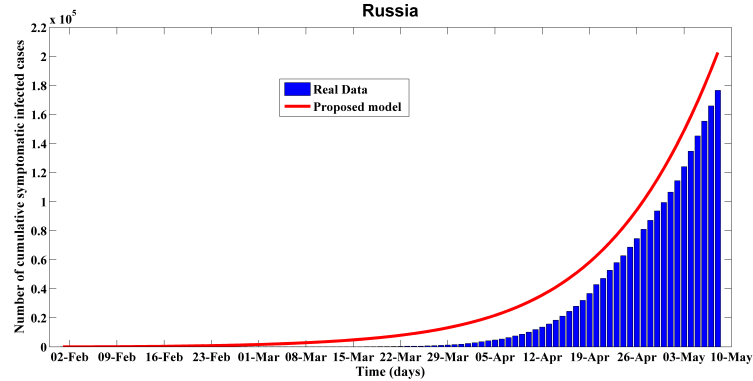
228 As we can see the results from the proposed model match the real data very well.
 229 Based on the proposed model, we want to project that from Figure 3, the number of
 230 daily detected symptomatic infectious cases in Russia will reach the peak at May 27
 231 with about 15.774K cases. As time progresses, our estimated daily projected mean
 232 error drops to 10% for the cumulative cases and daily new cases which represents the
 233 robustness of the model forecasting. The basic reproduction number is 4.234 as of May
 234 08, which lies in prior established findings 2 – 7 for COVID-19 Liu et al., (2020). The
 235 number of cumulative infected cases is projected to reach 970K around August 30, and
 236 the estimated total death cases will reach to about 35K in the end. To date, Russia’s
 237 official death toll of 1,827 is relatively low because not all deaths of people who have
 238 contracted the virus are being counted as Covid-19 deaths. Table 2 illustrates the key
 239 features used to calibrate this scenario which are compatible with the previous clinical
 240 studies and relevant literature.

Parameter	TRR input	lb	ub	TRR output	References
β	0.4	0.2	1.5	0.4852	Shen et al. (2020); Li et al., (2020)
λ	0.45	0.4	0.6	0.5249	Li et al., (2020); Ferguson et al., (2020)
r_1	0.76	0.1	0.999	0.9810	Estimated
r_2	0.03	0.01	0.9	0.0224	Estimated
η	0.05	0.01	0.9	0.0779	Estimated
κ	0.196	1/14	1/3	0.2443	Li et al., (2020); Lauer et al., (2020)
σ_1	0.01	0.0001	0.9	0.0067	Li et al., (2020); Ferguson et al., (2020)
σ_2	0.5	0.01	0.95	0.6894	Estimated
γ	0.3	0.1	0.9	0.7297	Ferguson et al., (2020); Zhou et al., (2020)
ϕ_D	0.1428	1/30	1/3	0.3332	Tang et al., (2020); Zhou et al., (2020)
ϕ_U	0.1428	1/30	1/3	0.0401	Tang et al., (2020); Zhou et al., (2020)
ϕ_H	0.1428	1/30	1/3	0.0433	Tang et al., (2020); Zhou et al., (2020)
δ_U	0.09	0.001	0.01	0.0013	Ferguson et al., (2020)
δ_H	0.09	0.001	0.01	0.0095	Ferguson et al., (2020)
q	0.015	0.01	0.5	0.0107	Estimated

Table 2: Necessary parameters for trust-region-reflective algorithm and for the Figure 3 calibrated response

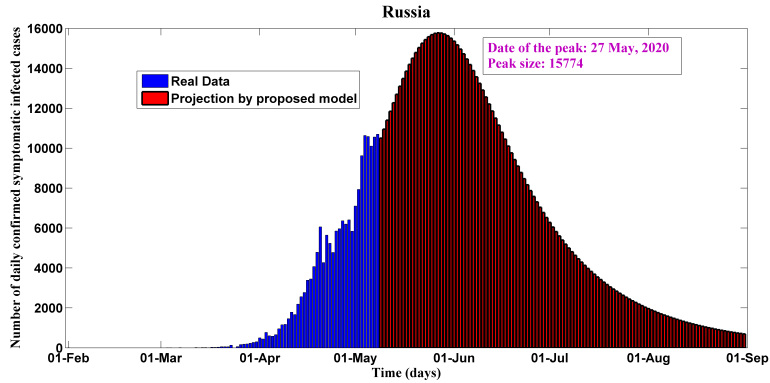


(a) Daily detected symptomatic infectious cases fitted from early February to early May, 2020

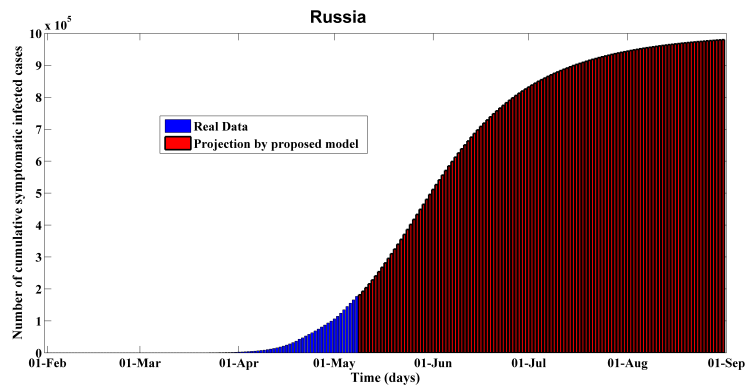


(b) Daily cumulative detected symptomatic infectious cases fitted from early February to early May, 2020

Figure 2: Fitting performance of calibrated $SEI_D I_U QHRD$ model for Russia from February 1 to May 08, 2020



(a) Daily detected symptomatic infectious cases calibrated and projected for Russia from early February to late August, 2020



(b) Daily cumulative detected symptomatic infectious cases calibrated and projected for Russia from early February to late August, 2020

Figure 3: Predictions of the proposed $SEI_D I_U QHRD$ model for Russia from early March to late August, 2020

241 *5.2. Analysis and prediction for Brazil*

242 The coronavirus disease 2019 (COVID-19) pandemic headed toward Latin America
 243 later than other continents. On Feb 25, 2020, the first infected case was documented
 244 . But now, Brazil has surpassed the records in Latin America in terms of deaths and
 245 new infected cases (155939 cases and 10627 deaths as of May 9). This is probably an
 246 underestimated scenario in comparison to real severity in Brazil. Our analysis projects
 247 that Brazil is developing as one of the world’s next coronavirus hotspots. The model
 248 fitting and projection results for Brazil from late February to late August are shown
 249 in Figure 4 and 5. We took real data from February 25 to May 08 to calibrate the
 250 model parameters. As we can see the results from the proposed model fit the real data
 251 very well. Based on the proposed model, we project that from Figure 5, the number of
 252 daily detected symptomatic infectious cases in Brazil seem reaching the peak around
 253 June 11 with about 26.449K cases. The basic reproduction number is estimated about
 254 5.3467 as of May 11, which is in between the observed basic reproduction number
 255 for COVID-19, estimated about 2-7 for COVID-19 Liu et al., (2020). This crucial
 256 epidemiological parameter could blow up because of scant diagnostics and impermanent
 257 non-pharmaceutical interventions. The case-fatality rate is hovering around 9.3% as of
 258 May 11, which is necessary to assess how much community transmission has occurred

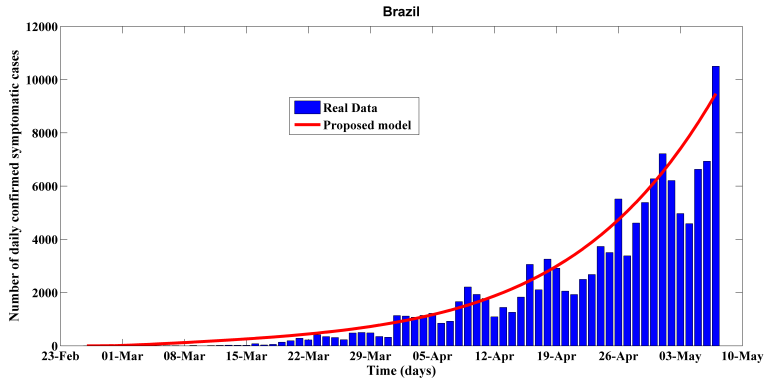
Parameter	TRR input	lb	ub	TRR output	References
β	0.3	0.2	1.5	0.5155	Shen et al. (2020); Li et al., (2020)
λ	0.45	0.4	0.6	0.5855	Li et al., (2020); Ferguson et al., (2020)
r_1	0.76	0.1	0.999	0.9855	Estimated
r_2	0.03	0.01	0.9	0.0159	Estimated
η	0.05	0.01	0.9	0.0897	Estimated
κ	0.196	1/14	1/3	0.1867	Li et al., (2020); Lauer et al., (2020)
σ_1	0.01	0.0001	0.9	0.0072	Moriarty et al., (2020); Verity et al., (2020)
σ_2	0.5	0.1	0.95	0.7308	Estimated
γ	0.3	0.1	0.9	0.7	Ferguson et al., (2020); Zhou et al., (2020)
ϕ_D	0.1428	1/30	1/3	0.3333	Tang et al., (2020); Zhou et al., (2020)
ϕ_U	0.1428	1/30	1/3	0.0356	Tang et al., (2020); Zhou et al., (2020)
ϕ_H	0.1428	1/30	1/3	0.0431	Tang et al., (2020); Zhou et al., (2020)
δ_U	0.09	0.001	0.01	0.001	Ferguson et al., (2020)
δ_H	0.09	0.001	0.01	0.009	Ferguson et al., (2020)
q	0.015	0.01	0.5	0.04	Estimated

Table 3: Necessary parameters for trust-region-reflective algorithm and for the Figure 5 calibrated response

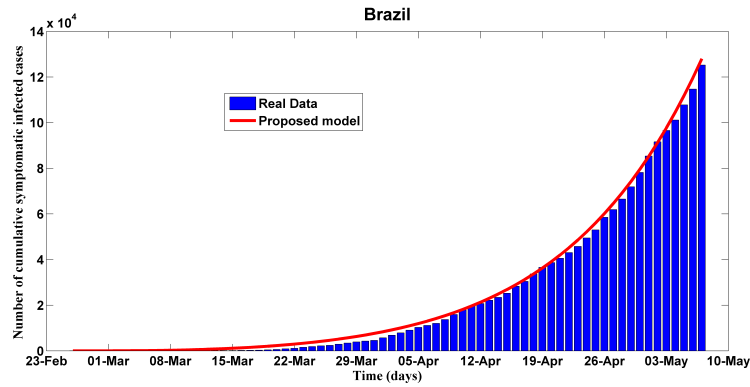
and its burden. According to our projection, this ratio could be doubled within two months. The number of cumulative infected cases is projected to reach 1800K around August 30 if current trend is held, and the estimated total death cases will reach to about 108K in the end. Table 3 illustrates the key features used to calibrate this scenario which are compatible with the previous clinical studies and relevant literature.

5.3. Analysis and prediction for India

Some people might think about the possibilities of the presence of a less virulent strain of the virus in India, along with the possibility that its hot weather could diminish the contagion. Nevertheless, our mathematical analysis suggests that India could become the new Covid-19 hotspot in South Asia. According to our projection, India could continue seeing spikes in the number of cases as it time progresses despite of following lockdown and other disease mitigation measures. The first case of the COVID-19 pandemic in India was reported on 30 January 2020, originating from China. But now, India has the most cases and deaths in South Asia (62,808 cases and 2,101 deaths as of May 9), and these are probably substantial underestimates. Figure 6 and 7 illustrate COVID-19 disease modeling and prediction for India from late January to late August. We took real-time data from January 30 to May 8 to calibrate the model parameters. As we can see, our proposed model match well for the historical real data. Based on our prediction from Figure 7, the number of daily detected symptomatic infectious cases in India seem reaching the peak around June 15 with about 9.504K cases. The basic reproduction number is 5.218 as of May 11, which lies between the studied observations Liu et al., (2020). This estimation may be considered as an overestimation of this critical parameter. Notwithstanding, this is owing to the infectiousness factor of the asymptomatic spreaders. Minimally or reasonably symptomatic infectious and the asymptomatic spreaders should be quarantined to avoid the transmission of the virus, with the critically symptomatic patients isolated



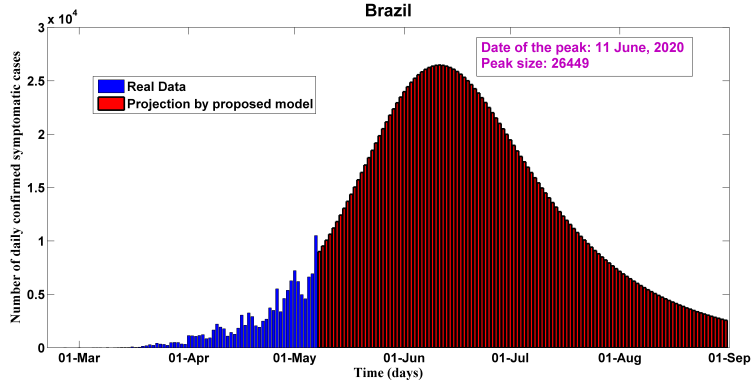
(a) The number of daily detected symptomatic infectious cases measured and fitted from late February to early May, 2020



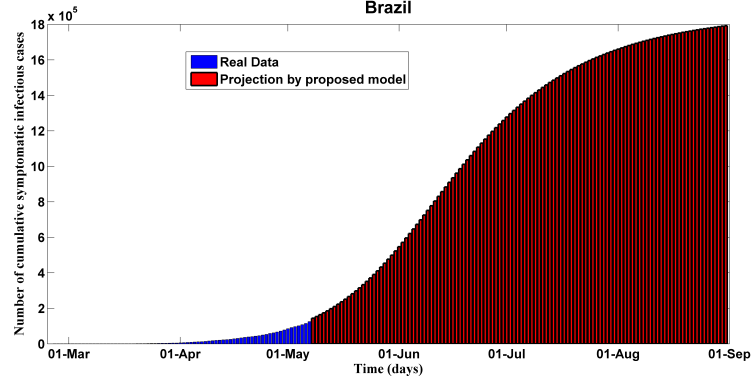
(b) The number of cumulative detected symptomatic infectious cases cases measured and fitted from late February to early May, 2020

Figure 4: Fitting performance of calibrated $SEI_{DU}QHRD$ model for Brazil from 26 February to 8 May, 2020

285 in proper health care settings. By carrying out massive scale contract tracing, risky
 286 individuals could be identified by means of their exposure. The number of cumulative
 287 infected cases is projected to reach 730K around August 30 if current pattern is held,
 288 and the estimated total death cases will reach to about 43.8K in the end. Table 4
 289 illustrates the key features used to calibrate this scenario which are compatible with
 290 the previous clinical studies and relevant literature. Interestingly, we have found in our
 291 analysis that India’s case-fatality rate is at 3.5% and the country’s recovery rate is at
 292 33% which commensurate with real reported statistics precisely.



(a) The number of daily detected symptomatic infectious cases measured and projected for Brazil from late February to late August, 2020

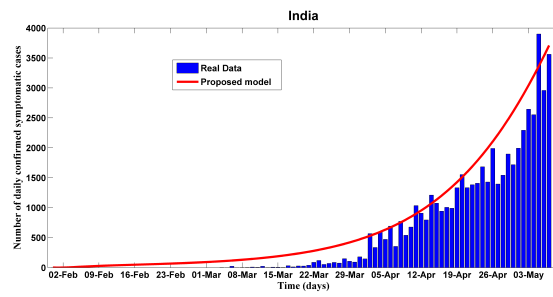


(b) The number of cumulative detected symptomatic infectious cases measured and projected for Brazil from late February to late August, 2020

Figure 5: Predictions of the proposed $SEI_D I_U QHRD$ model for Brazil from late February to late August, 2020

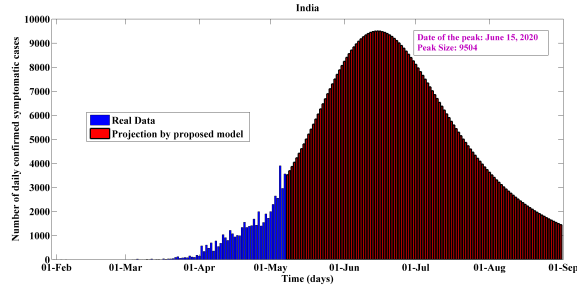
Parameter	TRR input	lb	ub	TRR output	References
β	0.3	0.2	1.5	0.3995	Shen et al. (2020); Li et al., (2020)
λ	0.4	0.4	0.6	0.5995	Li et al., (2020); Ferguson et al., (2020)
r_1	0.76	0.1	0.999	0.9911	Estimated
r_2	0.03	0.01	0.9	0.01	Estimated
η	0.05	0.01	0.9	0.0997	Estimated
κ	0.196	1/14	1/3	0.3296	Li et al., (2020); Lauer et al., (2020)
σ_1	0.01	0.0001	0.1	0.00046	Moriarty et al., (2020); Verity et al., (2020)
σ_2	0.5	0.1	0.95	0.7495	Estimated
γ	0.3	0.1	0.9	0.8	Ferguson et al., (2020); Zhou et al., (2020)
ϕ_D	0.1428	1/30	1/3	0.3333	Tang et al., (2020); Zhou et al., (2020)
ϕ_U	0.1428	1/30	1/3	0.0334	Tang et al., (2020); Zhou et al., (2020)
ϕ_H	0.1428	1/30	1/3	0.3335	Tang et al., (2020); Zhou et al., (2020)
δ_U	0.09	0.001	0.01	0.001	Ferguson et al., (2020)
δ_H	0.09	0.001	0.01	0.01	Ferguson et al., (2020)
q	0.015	0.01	0.5	0.0507	Estimated

Table 4: Necessary parameters for trust-region-reflective algorithm and for the Figure 7 calibrated response

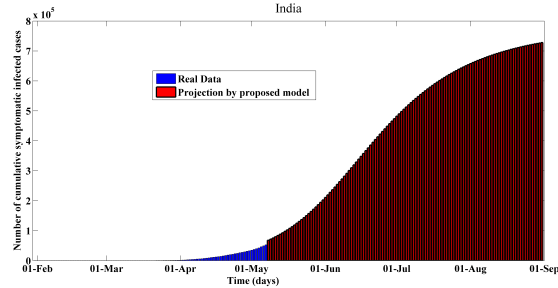


(a) The number of daily detected symptomatic infectious cases measured and fitted from early March to early May, 2020

Figure 6: Fitting performance of calibrated $SEI_D I_U QHRD$ model for India from 8 March to early May, 2020



(a) The number of daily detected symptomatic infectious cases measured and projected for India from late January to late August, 2020



(b) The number of cumulative detected symptomatic infectious cases measured and projected for India from early March to late August, 2020

Figure 7: Predictions of the proposed $SEI_D I_U QHRD$ model for India from late January to late August, 2020

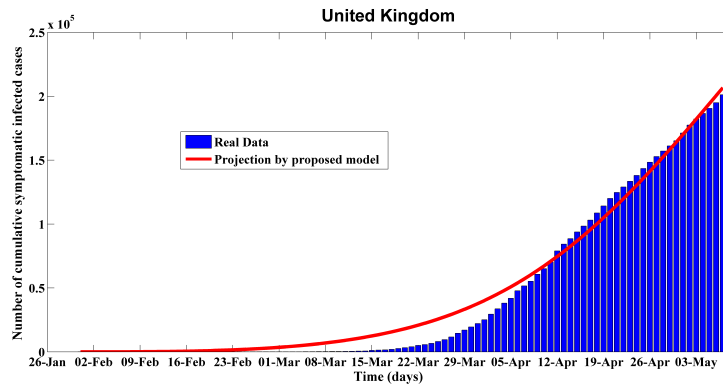
5.4. Analysis and prediction for the United Kingdom

Our analysis indicates that the United Kingdom could face risk of a second wave of coronavirus infections as the United Kingdom gradually eases a nationwide lockdown. According to [Worldometer, \(2020\)](#), by 11 May there had been 223,060 confirmed cases and 32,065 deaths overall a rate of 465 deaths per million population. The outbreak in London has the highest number and highest rate of infections, while England and Wales are the UK countries with the highest recorded death rate per capita. Recently, The prime minister of the UK has expressed his plan to unveil a coronavirus warning system as an intervention strategy, while he was planning to ease the lockdown gradually in the UK. For the UK, the modeling and projection results from January 31 to August 31 are shown in Figure 8 and 9. As we can see from Figure 9, the number of daily detected symptomatic infectious cases reached the peak around April 10. Since then the curve has been maintaining a plateau which is a really unusual scenario. This phenomenon has closely been captured by our proposed model. This case study was really important for the validation of our model. In fact, this guarantees the fact that this model is capable of providing more precise and vigorous short-term predictions of COVID-19 dynamics. According to our calculation, the basic reproduction number is around 4.649 as of May 09, which lies in the prior studies of COVID-19 [Anastassopoulou et al., \(2020\)](#); [Liu et al., \(2020\)](#). The number cumulative infected cases is projected to reach 618K around August 30, and the estimated total death cases will reach to about 63.48K in the above mentioned period. Importantly, as of May 11, we have found in our analysis that the UK's case-fatality rate is at 17.2%, which is the worst among our five studied cases. This could exacerbate as time progresses in the absence of proven

Parameter	TRR input	lb	ub	TRR output	References
β	0.3	0.2	1.5	0.73	Shen et al. (2020); Li et al., (2020)
λ	0.4	0.4	0.6	0.59	Li et al., (2020); Ferguson et al., (2020)
r_1	0.76	0.6	0.999	0.97	Estimated
r_2	0.03	0.01	0.1	0.024	Estimated
η	0.05	0.04	0.1	0.09	Estimated
κ	0.196	1/14	1/3	0.3333	Li et al., (2020); Lauer et al., (2020)
σ_1	0.01	0.0001	0.01	0.0044	Moriarty et al., (2020); Verity et al., (2020)
σ_2	0.5	0.3	0.95	0.37	Estimated
γ	0.3	0.1	0.9	0.79	Ferguson et al., (2020); Zhou et al., (2020)
ϕ_D	0.1428	1/30	1/3	0.3333	Tang et al., (2020); Zhou et al., (2020)
ϕ_U	0.1428	1/30	1/3	0.0542	Tang et al., (2020); Zhou et al., (2020)
ϕ_H	0.1428	1/30	1/3	0.0333	Tang et al., (2020); Zhou et al., (2020)
δ_U	0.09	0.001	0.01	0.001	Ferguson et al., (2020)
δ_H	0.09	0.001	0.01	0.001	Ferguson et al., (2020)
q	0.015	0.01	0.5	0.015	Estimated

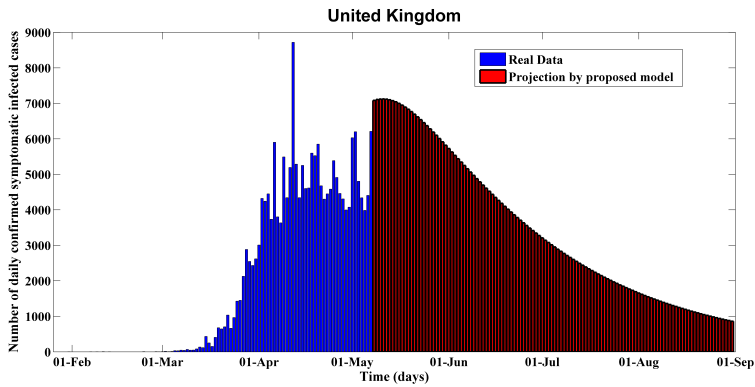
Table 5: Necessary parameters for trust-region-reflective algorithm and for the Figure 9 calibrated response

316 effective therapy or a vaccine. In addition, Our study suggests that relaxing social
317 distancing too soon could result in thousands of additional death in the UK. Table 5
318 illustrates the key features used to calibrate this scenario which are compatible with
319 the previous clinical studies and relevant literature.

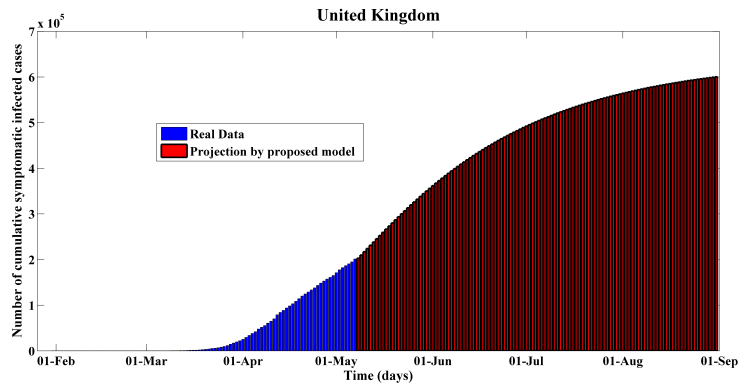


(a)

Figure 8: Fitting performance of calibrated $SEI_D I_U QHRD$ model for the United Kingdom from 31 January to early May, 2020



(a) The number of daily detected symptomatic infectious cases measured and projected for the United Kingdom from late January to late August, 2020



(b) The number of cumulative detected symptomatic infectious cases measured and projected for India from late January to late August, 2020

Figure 9: Predictions of the proposed $SEI_D I_U QHRD$ model for the United Kingdom from late January to late August, 2020

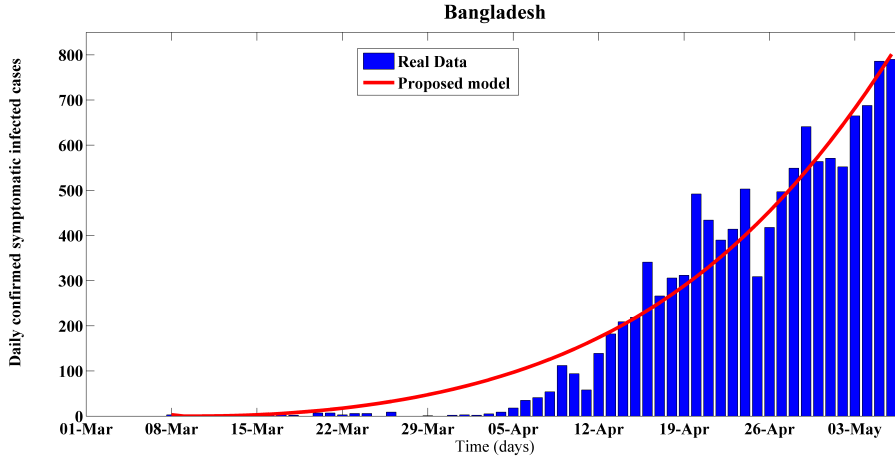
Parameter	TRR input	lb	ub	TRR output	Reference
β	0.3	0.2	1.5	0.3972	Shen et al. (2020); Li et al., (2020)
λ	0.4	0.4	0.6	0.5498	Li et al., (2020); Ferguson et al., (2020)
r_1	0.76	0.1	0.999	0.9454	Estimated
r_2	0.03	0.01	0.9	0.02	Estimated
η	0.05	0.01	0.9	0.06	Estimated
κ	0.196	1/14	1/3	0.0714	Li et al., (2020); Lauer et al., (2020)
σ_1	0.01	0.0001	0.9	0.001	Moriarty et al., (2020); Verity et al., (2020)
σ_2	0.5	0.3	0.98	0.95	Estimated
γ	0.3	0.1	0.9	0.5	Ferguson et al., (2020); Zhou et al., (2020)
ϕ_D	0.1428	1/30	1/3	0.3333	Tang et al., (2020); Zhou et al., (2020)
ϕ_U	0.1428	1/30	1/3	0.0333	Tang et al., (2020); Zhou et al., (2020)
ϕ_H	0.1428	1/30	1/3	0.3275	Tang et al., (2020); Zhou et al., (2020)
δ_U	0.09	0.001	0.01	0.0011	Ferguson et al., (2020)
δ_H	0.09	0.001	0.01	0.01	Ferguson et al., (2020)
q	0.015	0.01	0.5	0.012	Estimated

Table 6: Necessary parameters for trust-region-reflective algorithm and for the Figure 11 calibrated response

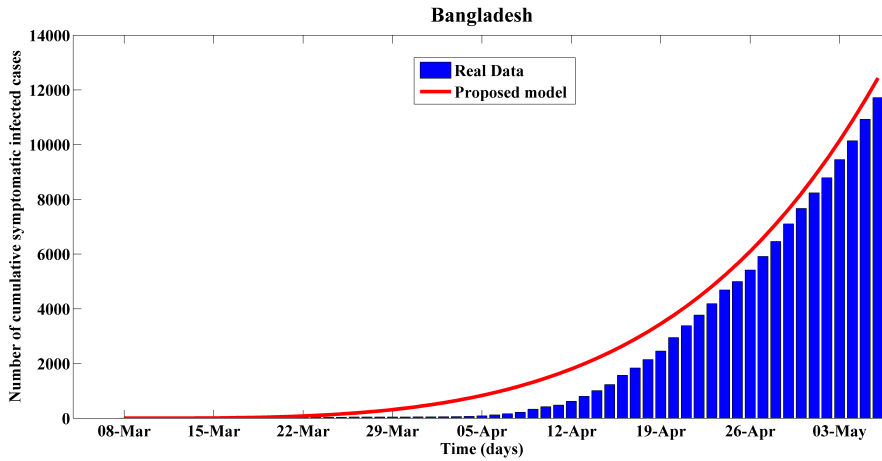
5.5. Analysis and prediction for Bangladesh

For Bangladesh, the calibration and projection results from early March to late August of are shown in Figure 10 and Figure 11. On 22 March, with an aim to curtail the spread of the novel coronavirus in the wake of four deaths and at least 39 infections, Bangladesh government deployed a nationwide lockdown effective from 26 March, 2020. Notice that, there are some jumps in the number of confirmed daily new infected cases data from 16 april to 20 april due to the increase of limited testing system (from 2000 samples to 2700 samples per day) Institute of Epidemiology, Disease Control and Research (IEDCR). Bangladesh is still struggling (around 6700 samples per day) Institute of Epidemiology, Disease Control and Research (IEDCR) to design a massive scale testing program as of May 11, 2020. Despite the fact, as we can see from Figure 10, our proposed model fits well for the historical real-time data. As time progresses, the estimated error declines and is hovering around 10% for the cumulative cases and daily new cases according to our calculated daily projected mean error. The estimated case-fatality rate in Bangladesh is at 2.7% which is kind of satisfactory, however without massive scale testing this rate could rise sharply incoming days. Moreover, the country’s estimated recovery rate is at 24% which again complements the real statistics precisely. Importantly, without an aggressive level mass-testing program it is impossible to portray the real outbreak scenario in Bangladesh. Table 6 illustrates the key features used to calibrate this scenario which are compatible with the previous clinical studies and relevant literature.

On 4 May, Bangladesh authorities intended to open up more factories, shopping malls and logistics operations, as they could diminish the economic impact of a coronavirus lockdown which they extended to May 16 Ministry of Health & Family Welfare of Bangladesh, (2020). This ease of lockdown could worsen the ongoing community transmission drastically. As we can see form Figure 11, the daily detected symptomatic infected cases (confirmed) will reach the peak (about 2209) around June 11, 2020 and



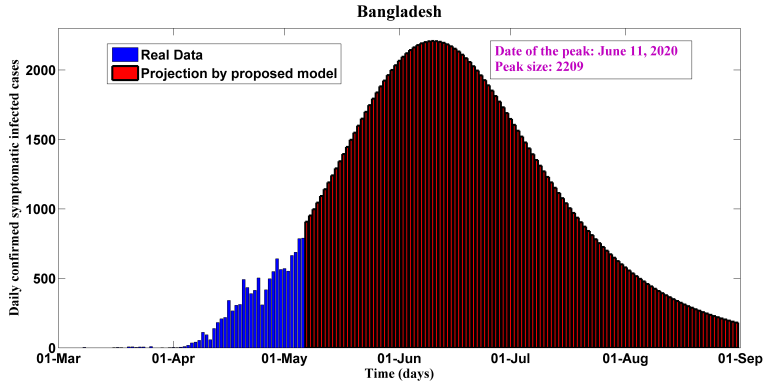
(a) The number of daily detected symptomatic infectious cases measured and fitted from early March to early May, 2020



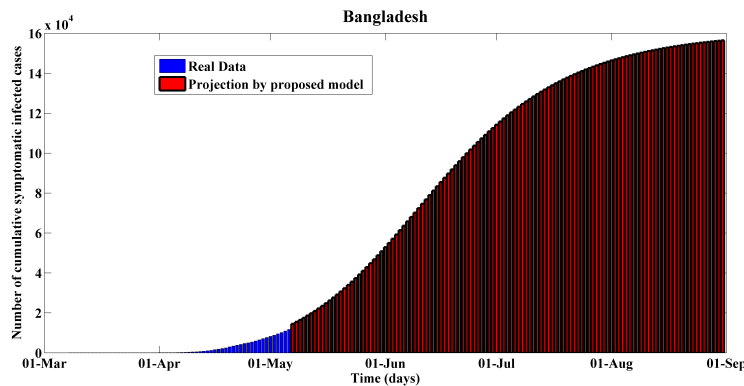
(b) The number of cumulative detected symptomatic infectious cases measured and fitted from early March to early May, 2020

Figure 10: Fitting performance of calibrated $SEI_D I_U QHRD$ model for Bangladesh from 8 March to early May, 2020

347 then start to de-escalate. However, the probable peak time could occur in no time due
 348 to easing the coronavirus lockdown too quickly and this could bring a second wave of
 349 infections in the outbreak after post-peak period. The effective reproduction number is
 350 around 3.5 as of May 11, which again lies in prior established ranges [Anastassopoulou](#)
 351 [et al., \(2020\)](#); [Liu et al., \(2020\)](#). Our estimation is reasonably high which due to the
 352 fact that we have considered the infectiousness factor of the asymptomatic carriers.
 353 Massive level testing is highly required and recommended to identify the asymptomatic
 354 spreaders quickly. Unlike other mitigation strategies like reporting contacts, putting on
 355 face masks, and maintaining physical distancing, a massive test-and-isolate approach
 356 could control the disease burden of COVID-19. Otherwise, this basic reproduction
 357 number could increase upto 5.7 within 20 days and inhabitants of Bangladesh could
 358 see a disease catastrophe in near future. In near future, owing to various changing
 359 factors such as mitigation measures and mass people awareness such estimation and
 360 projection could differ significantly.



(a) The number of daily detected symptomatic infectious cases measured and projected for Bangladesh from early March to late August, 2020



(b) The number of cumulative detected symptomatic infectious cases measured and projected for Bangladesh from early March to late August, 2020

Figure 11: Predictions of the proposed $SEI_D I_U QHRD$ model for Bangladesh from early March to late August, 2020

361 6. Global Sensitivity Analysis

362 PRCC analysis which is a global sensitivity analysis method that calculates the
 363 partial rank correlation coefficient for the model inputs (sampled by Latin hypercube
 364 sampling method) and outputs [Marino et al., \(2008\)](#); [Blower et al., \(1994\)](#); [Nabi et](#)
 365 [al., \(2020\)](#). The PRCC method assumes a monotonic relationship between the model
 366 input parameters and the model outputs.

367 The calculated PRCC values are between -1 and 1 and they are comparable among
 368 different model inputs. Quantitative relationship between the model input and model
 369 response can be determined by calculating the PRCC values. A positive PRCC value
 370 depicts that the model output can be increased by increasing the respective model
 371 input parameter or vice versa. In addition, a negative PRCC value indicates a neg-
 372 ative correlation between the model input and output. The magnitude of the PRCC
 373 sensitivity measures the significance of the model input in contributing to the model
 374 output.

375 As our proposed epidemic model contains a moderate number of empirical param-
 376 eters, uncertainty analysis can give considerable insights regarding the quantitative re-
 377 lationship between model responses and model input parameters. However, it is really
 378 challenging for complex models to determine the relationship with sufficient accuracy.

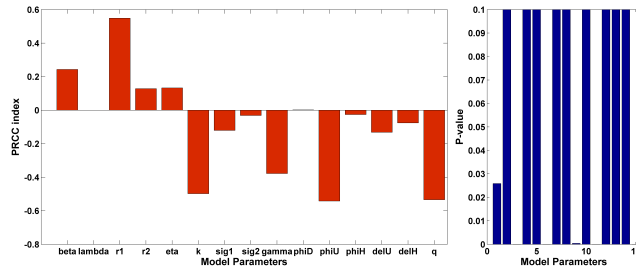
379 Importantly, we have got startling yet realistic results from our sensitivity analysis.
380 As we can see from Figure 12, we found nearly the same qualitative and significant
381 quantitative relationship between the number of symptomatic infectious individuals
382 (one of the crucial model responses) and three parameters which are rate of getting
383 quarantined of susceptible individuals (q), transition rate from exposed to infectious
384 or quarantined (κ) which can also be referred as the inverse of the average incuba-
385 tion period of COVID-19 and recovery rate of undetected asymptomatic (undetected)
386 infectious carriers for our proposed model.

387 In case of Russia, from Figure 12a recovery rate of undetected asymptomatic car-
388 riers (ϕ_U) is the most negatively influential parameter when the number of detected
389 infectious individuals is our selected model response. The PRCC index is found to
390 be -0.585 . In addition, rate of entering into home-quarantine or self-quarantine of
391 susceptible individuals (q) and the fraction of wrongly quarantined people who be-
392 come susceptible after certain latent period (r_1) are the other two influential empirical
393 features with PRCC indexes are -0.5672 and 0.567 respectively.

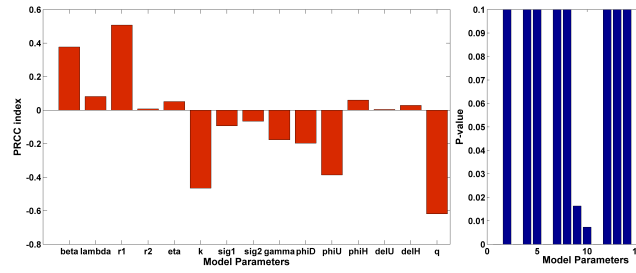
394 In case of Brazil, rate of getting home-quarantined or self-quarantined of suscep-
395 tible individuals (q), the fraction of quarantined people who become susceptible due
396 to avoiding home-quarantine (r_1), and the inverse of the COVID-19 mean latent peri-
397 od are the most influential parameter on the symptomatic infectious population size
398 ($I_D(t)$). The corresponding PRCC indices are -0.62 , 0.53 and -0.499 . The figure 12b
399 qualitatively elucidates that a high quarantine rate of the susceptible individuals can
400 curtail the number of symptomatic infected individuals. In broader view, high efficacy
401 of home or self-quarantine and a lower unlockdown rate could flatten the $I_D(t)$ curve
402 in Brazil.

403 In case of the India, rate of getting home-quarantined or self-quarantined of sus-
404 ceptible individuals (q) and the inverse of the COVID-19 incubation period are the
405 most influential parameter on the symptomatic infectious population size ($I_D(t)$) and
406 the corresponding PRCC indexes are -0.64 and -0.62 . Both the parameters are neg-
407 atively sensitive to the size of detected infected individuals which is illustrated in the
408 figure 12c. This elucidates that a higher quarantine rate of the susceptible individuals
409 can reduce the number of symptomatic infected individuals. Therefore, it is obvious
410 that early unlockdown in India could worsen the outbreak situation in the blink of an
411 eye.

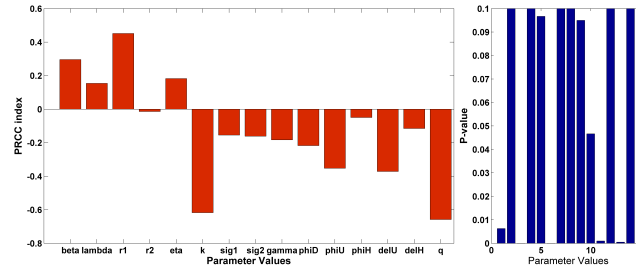
412 In case of the UK, rate of getting home-quarantined or self-quarantined of suscep-
413 tible individuals (q) and the inverse of the COVID-19 incubation period are the most
414 influential parameter on the symptomatic infectious population size ($I_D(t)$) and the
415 corresponding PRCC indices are -0.58 and -0.499 . Both the parameters are nega-
416 tively sensitive to the size of detected infected individuals which is illustrated in the
417 figure 12d. This elucidates that a higher quarantine rate of the susceptible individuals
418 can curtail the number of symptomatic infected individuals. Nevertheless, early easing
419 lockdown measures could bring a second wave of infection in the UK in no time.



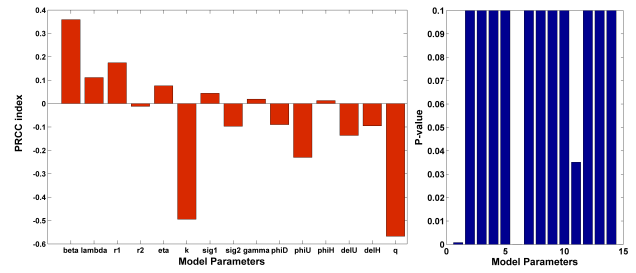
(a) Sensitivity analysis for Russia



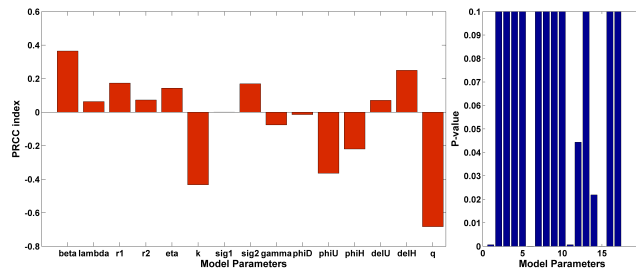
(b) Sensitivity analysis for Brazil



(c) Sensitivity analysis for India



(d) Sensitivity analysis for the UK



(e) Sensitivity analysis for Bangladesh

Figure 12: Sensitivity of the symptomatic infected cases while changing parameters in the proposed $SEI_D I_U QRHD$ model as indicated by the PRCC index for five different countries

420 For Bangladesh, it has been found in our analysis, home-quarantine rate is the most
421 negatively sensitive parameter on the size of symptomatic infectious individuals and the
422 corresponding PRCC index is -0.68 which is the highest among our five studied cases.
423 The result in Figure 12e elucidates that if the people in Bangladesh start breaking
424 social distancing restrictions extensively, then it would be difficult to control the disease
425 outbreak there. As of May 11, when Bangladesh is seeing continuous spikes in COVID-
426 19 infections every day, the government has announced an easing of movement for all
427 on a limited scale with a view to reviving the country's economy. Moreover, the length
428 of the inverse of the latent period is the another negatively sensitive parameter with
429 PRCC index lying at -0.43 .

430 7. Concluding Remarks

431 We have proposed a methodology for the calibration of the key epidemiological
432 parameters as well as forecasting of the outbreak dynamics of COVID-19 pandemic
433 in Russia, Brazil, India, Bangladesh and the UK, while considering publicly available
434 data from late January 2020 to early May 2020 with an introduction of an real-time
435 differential $SEI_D I_U QHRD$ epidemic model which can give more accurate, realistic and
436 precise short-term predictions. Baseline parameter ranges are chosen from the recent
437 clinical studies and relevant literature concerning the COVID-19 infection. Trust-
438 region-reflective algorithm which is one of the robust least-squares fitting techniques,
439 has been deployed to calibrate the proposed model parameters. Numerical results on
440 the recent COVID-19 data from Russia, Brazil, India, Bangladesh and the UK have
441 been analyzed with an aim to determine probable peak dates and sizes for the above
442 mentioned countries. Based on the projection as of May 11, 2020, Russia will reach
443 the peak in terms of daily infected cases and death cases around end of May. Brazil
444 and India will reach the peak in terms of daily symptomatic infectious cases and death
445 cases around beginning of June. In addition, the United Kingdom might face a second
446 wave of infection provided that lockdown is lifted quickly. Global sensitivity analysis
447 results depict that home-quarantine or self-quarantine is the most effective measure for
448 controlling the transmission and spread of the novel coronavirus infection. To fade out
449 the pandemic, it is compulsory to identify potential carriers and asymptomatic infec-
450 tious spreaders through and massive scale testing scheme and without sufficient level
451 of evidence of controlled low transmission rate of COVID-19 in any certain territory,
452 we cannot afford lifting up physical distancing measures.

Declarations

Competing interests: The authors declare no competing interests.

453 **References**

- 454 Shen, M., Peng, Z., Xiao, Y., & Zhang, L. (2020). Modelling the epidemic trend of the
455 2019 novel coronavirus outbreak in China. *bioRxiv*.
- 456 Read, J. M., Bridgen, J. R., Cummings, D. A., Ho, A., & Jewell, C. P. (2020). Novel
457 coronavirus 2019-nCoV: early estimation of epidemiological parameters and epidemic
458 predictions. *MedRxiv*.
- 459 Li, R., Pei, S., Chen, B., Song, Y., Zhang, T., Yang, W., & Shaman, J. (2020). Substan-
460 tial undocumented infection facilitates the rapid dissemination of novel coronavirus
461 (SARS-CoV2), *Science*, 368(6490), 489-493.
- 462 Ferguson, N., Laydon, D., Nedjati Gilani, G., Imai, N., Ainslie, K., Baguelin, M., &
463 Dighe, A. (2020). Report 9: Impact of non-pharmaceutical interventions (NPIs) to
464 reduce COVID19 mortality and healthcare demand.
- 465 Lauer, S. A., Grantz, K. H., Bi, Q., Jones, F. K., Zheng, Q., Meredith, H. R., &
466 Lessler, J. (2020). The incubation period of coronavirus disease 2019 (COVID-19)
467 from publicly reported confirmed cases: estimation and application. *Annals of inter-
468 nal medicine*, 172(9), 577-582.
- 469 Tang, B., Bragazzi, N. L., Li, Q., Tang, S., Xiao, Y., & Wu, J. (2020). An updated
470 estimation of the risk of transmission of the novel coronavirus (2019-nCov). *Infectious
471 Disease Modelling*, 5, 248–255.
- 472 Zhou, F., Yu, T., Du, R., Fan, G., Liu, Y., Liu, Z., & Guan, L. (2020). Clinical course
473 and risk factors for mortality of adult inpatients with COVID-19 in Wuhan, China:
474 a retrospective cohort study. *The Lancet*, 395 (10229), 1054-1062.
- 475 Moriarty, L. F., Plucinski, M., M., Marston, & B. J. et al. (2020). Public Health
476 Responses to COVID-19 Outbreaks on Cruise Ships-Worldwide, February-March
477 2020. *Morbidity and Mortality Weekly Report*, 69, 347-352.
- 478 Wu, J. T., Leung, K., & Leung, G. M. (2020). Nowcasting and forecasting the potential
479 domestic and international spread of the 2019-nCoV outbreak originating in Wuhan,
480 China: a modelling study. *The Lancet*, 395(10225), 689-697.
- 481 Calafiore, G. C., Novara, C., & Possieri, C. (2020). A Modified SIR Model for the
482 COVID-19 Contagion in Italy. *arXiv preprint arXiv: 2003.14391*.
- 483 Kucharski, A. J., Russell, T. W., Diamond, C., Liu, Y., Edmunds, J., Funk, S., &
484 Davies, N. (2020). Early dynamics of transmission and control of COVID-19: a
485 mathematical modelling study. *The Lancet Infectious Diseases*, 20(5), 553-558.
- 486 Simha, A., Prasad, R. V., & Narayana, S. (2020). A simple Stochastic SIR model for
487 COVID 19 Infection Dynamics for Karnataka: Learning from Europe. *arXiv preprint
488 arXiv:2003.11920*.

- 489 Anastassopoulou, C., Russo, L., Tsakris, A., & Siettos, C. (2020). Data-Based Analysis,
490 Modelling and Forecasting of the novel Coronavirus (2019-nCoV) outbreak. *PLOS*
491 *ONE*, 15(3), e0230405.
- 492 Nesteruk, I. (2020). Statistics based predictions of coronavirus 2019-nCoV spreading
493 in mainland China. MedRxiv.
- 494 Chang, S. L., Harding, N., Zachreson, C., Cliff, O. M., & Prokopenko, M. (2020).
495 Modelling transmission and control of the COVID-19 pandemic in Australia. arXiv
496 preprint arXiv:2003.10218.
- 497 Wilder, B., Charpignon, M., Killian, J. A., Ou, H. C., Mate, A., Jabbari, S., & Ma-
498 jumder, M. S. (2020). The Role of Age Distribution and Family Structure on COVID-
499 19 Dynamics: A Preliminary Modeling Assessment for Hubei and Lombardy. Avail-
500 able at SSRN 3564800.
- 501 Ruiz Estrada, M. A., & Koutronas, E. (2020). The Networks Infection Contagious Dis-
502 eases Positioning System (NICDP-System): The Case of Wuhan-COVID-19. Avail-
503 able at SSRN 3548413.
- 504 Center for Systems Science and Engineering at Johns Hopkins University. (2020).
505 COVID-19. Github Repository. <https://github.com/CSSEGISandData/COVID-19>.
506 Last accessed May 08, 2020.
- 507 Verity, R., Okell, L. C., Dorigatti, I., Winskill, P., Whittaker, C., Imai, N., & Dighe, A.
508 (2020). Estimates of the severity of coronavirus disease 2019: a model-based analysis.
509 *The Lancet Infectious Diseases*.
- 510 Diego Caccavo, Chinese and Italian COVID-19 outbreaks can be correctly described
511 by a modified SIRD model, MedRxiv.
- 512 Peter Turchin. Analyzing covid-19 data with sird models, (2020). [https://github.com/pturchin/CSH-Covid-19-Project/blob/master/Turchin_2020_](https://github.com/pturchin/CSH-Covid-19-Project/blob/master/Turchin_2020_Covid19.pdf)
513 [Covid19.pdf](https://github.com/pturchin/CSH-Covid-19-Project/blob/master/Turchin_2020_Covid19.pdf)
- 514
- 515 Hethcote, H. W., (2000). The Mathematics of Infectious Diseases, *SIAM Review*, 42(4),
516 599–653.
- 517 LaSalle, JP., (1976). The Stability of Dynamical Systems, *SIAM*, Regional Conference
518 Series in Applied Mathematics.
- 519 Van den Driessche, P., & Watmough, J., (2002). Reproduction numbers and sub-
520 threshold endemic equilibria for compartmental models of disease transmission,
521 *Mathematical biosciences*, 180(1-2), 29–48.
- 522 Diekmann, O., Heesterbeek, J. A. P., & Metz, J. A., (1990). On the definition and the
523 computation of the basic reproduction ratio R_0 in models for infectious diseases in
524 heterogeneous populations, *Journal of mathematical biology*, 28(4), 365–382.

- 525 Liu, Y., Gayle, A. A., Wilder-Smith, A. , & Rocklöv, J., (2020). The reproductive
526 number of COVID-19 is higher compared to SARS coronavirus. *Journal of Travel*
527 *Medicine*, 27(2).
- 528 Marino, S., Hogue, I. B., Ray, C. J., and Kirschner, D. E., (2008). A methodology for
529 performing global uncertainty and sensitivity analysis in systems biology, *Journal of*
530 *theoretical biology*, 254 (1), 178–196.
- 531 Blower, S. M., Dowlatabadi, H., (1994). Sensitivity and uncertainty analysis of
532 complex-models of disease transmission – an HIV model, as an example, *Int. Stat.*
533 *Rev.*, 62(2), 229–243.
- 534 Nabi, K. N. & Podder, C. N., (2020). Sensitivity analysis of chronic hepatitis C
535 virus infection with immune response and cell proliferation. *International Journal*
536 *of Biomathematics*, 13(3), 2050017.
- 537 Worldometer, <https://www.worldometers.info/coronavirus>, accessed: 12-05-2020.
- 538 Qianying, L., Shi, Z., Daozhou, G., Yijun, L., Shu, Y., Salihu, S. M., Maggie, H. W.,
539 Yongli, K., Weiming, W., Lin, Y., Daihai, H., (2020). A conceptual model for the
540 outbreak of Coronavirus disease 2019 (COVID-19) in Wuhan, China with individual
541 reaction and governmental action. *International Journal of Infectious Diseases*, 93,
542 211-216.
- 543 Institute of Epidemiology, Disease Control and Research (IEDCR), Bangladesh [https:](https://www.iedcr.gov.bd)
544 [//www.iedcr.gov.bd](https://www.iedcr.gov.bd), accessed: 11-05-2020.
- 545 Ministry of Health & Family Welfare of Bangladesh, [https://dghs.gov.bd/index.](https://dghs.gov.bd/index.php/en/home/5343-covid-19-update)
546 [php/en/home/5343-covid-19-update](https://dghs.gov.bd/index.php/en/home/5343-covid-19-update), accessed: 11-05-2020.

Figures

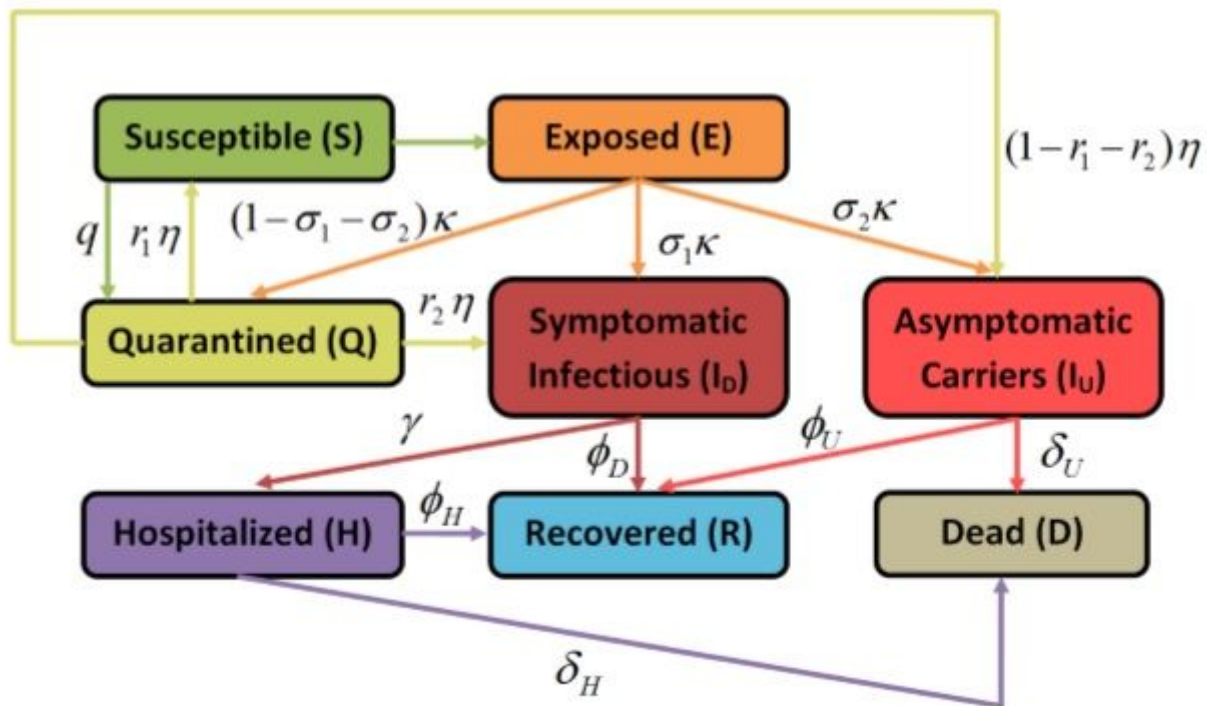
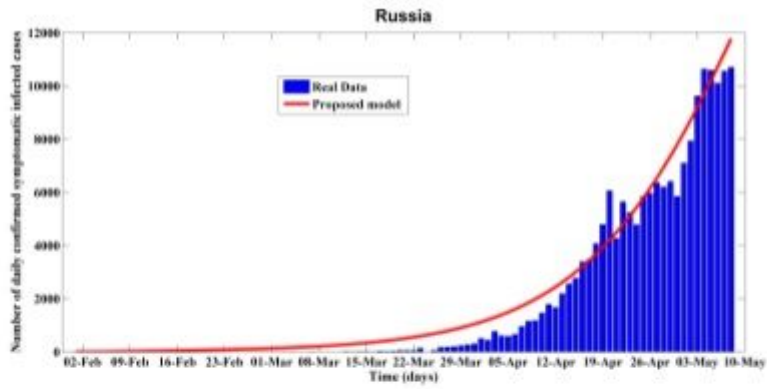
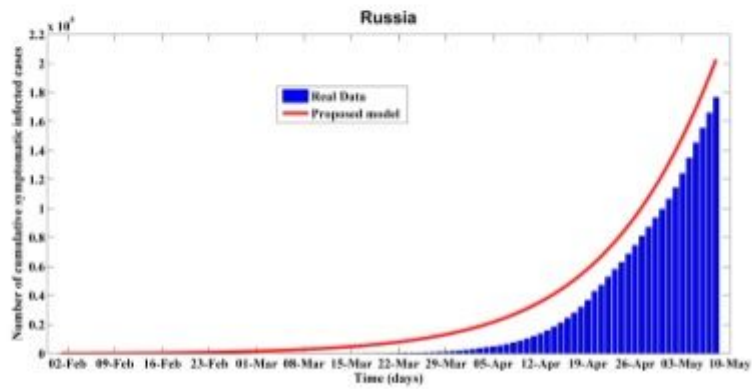


Figure 1

A schematic diagram that illustrates the proposed COVID-19 model



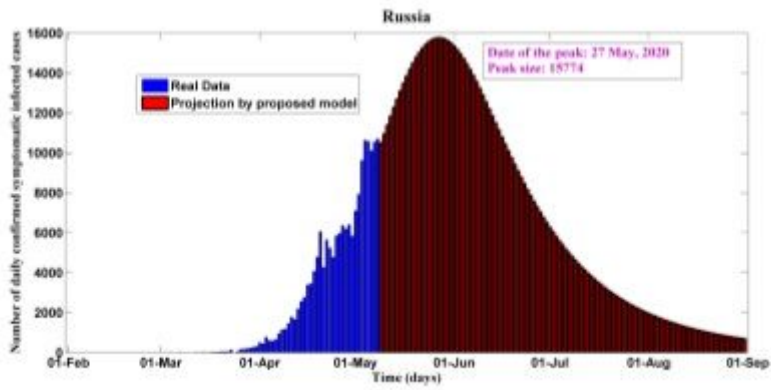
(a) Daily detected symptomatic infectious cases fitted from early February to early May, 2020



(b) Daily cumulative detected symptomatic infectious cases fitted from early February to early May, 2020

Figure 2

Fitting performance of calibrated SEIDUQHRD model for Russia from February 1 to May 08, 2020



(a) Daily detected symptomatic infectious cases calibrated and projected for Russia from early February to late August, 2020

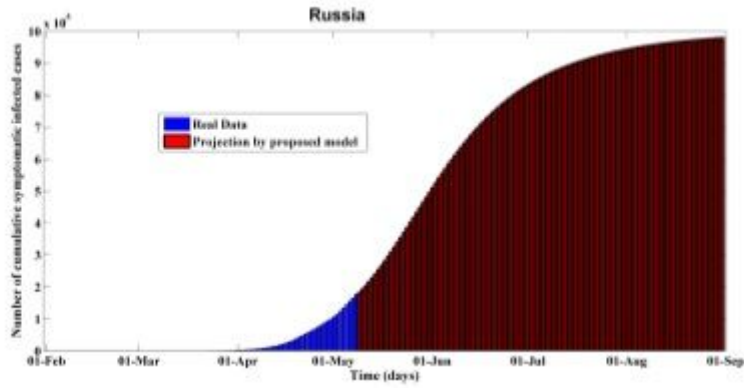
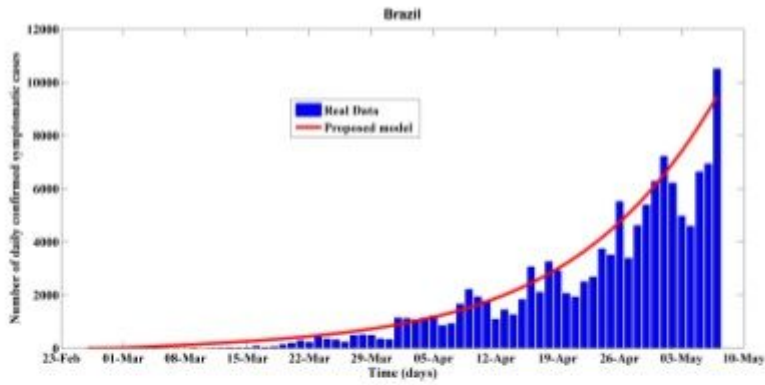
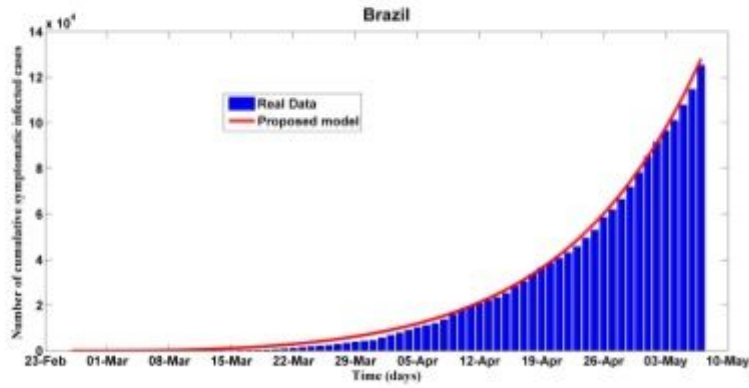


Figure 3

Predictions of the proposed SEIDIUQHRD model for Russia from early March to late August, 2020



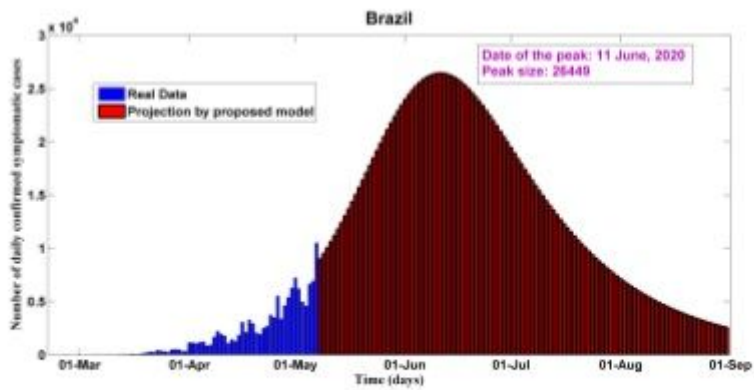
(a) The number of daily detected symptomatic infectious cases measured and fitted from late February to early May, 2020



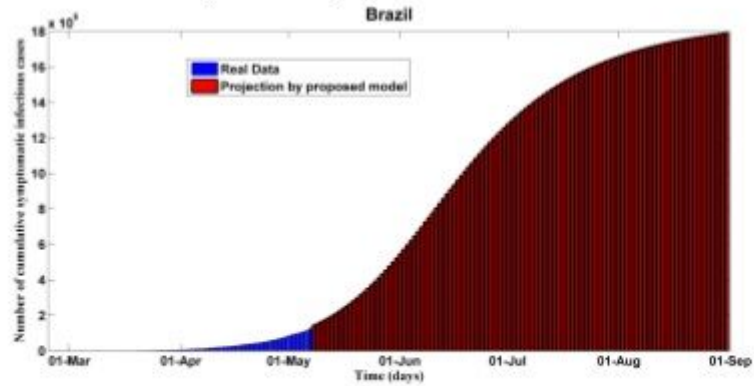
(b) The number of cumulative detected symptomatic infectious cases cases measured and fitted from late February to early May, 2020

Figure 4

Fitting performance of calibrated SEIDUQHRD model for Brazil from 26 February to 8 May, 2020



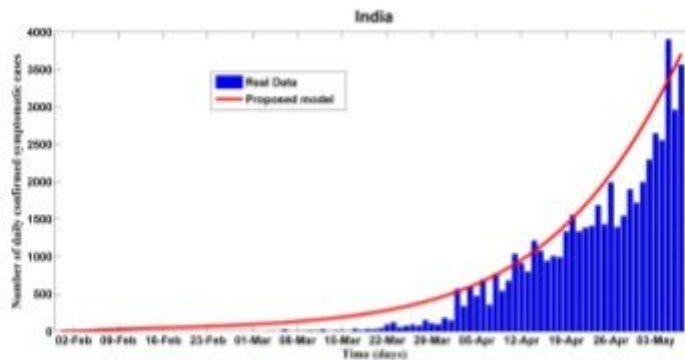
(a) The number of daily detected symptomatic infectious cases measured and projected for Brazil from late February to late August, 2020



(b) The number of cumulative detected symptomatic infectious cases measured and projected for Brazil from late February to late August, 2020

Figure 5

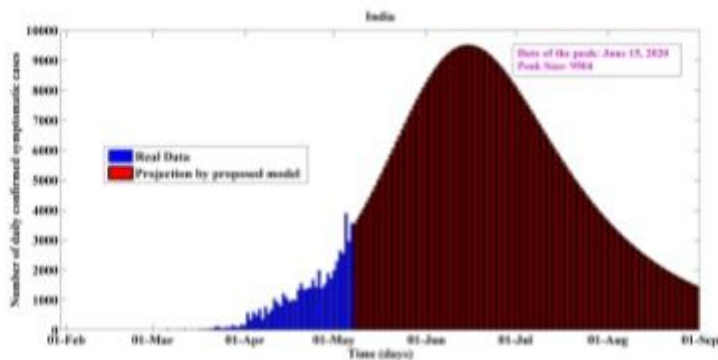
Predictions of the proposed SEIDIUQHRD model for Brazil from late February to late August, 2020



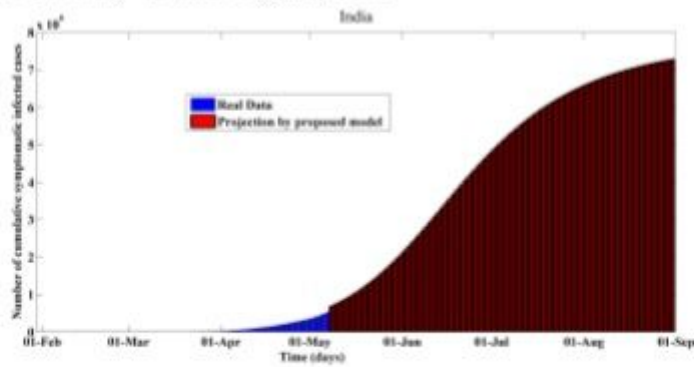
(a) The number of daily detected symptomatic infectious cases measured and fitted from early March to early May, 2020

Figure 6

Fitting performance of calibrated SEIDIUQHRD model for India from 8 March to early May, 2020



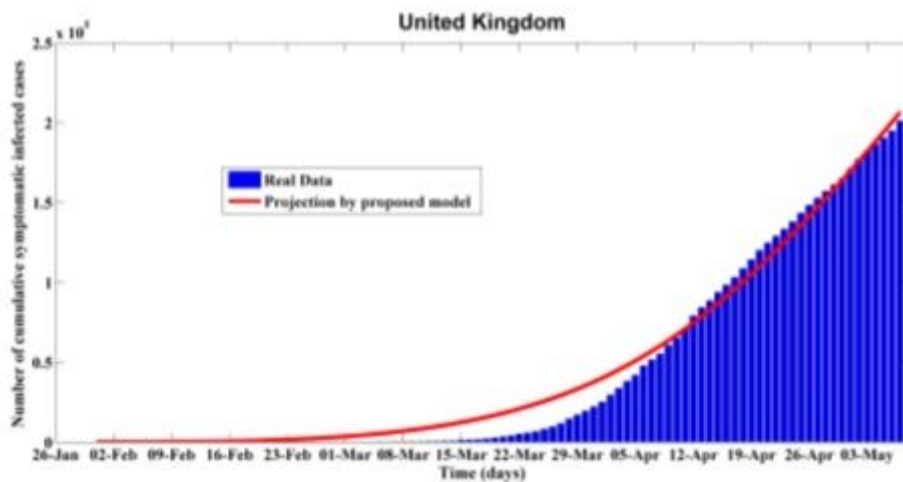
(a) The number of daily detected symptomatic infectious cases measured and projected for India from late January to late August, 2020



(b) The number of cumulative detected symptomatic infectious cases measured and projected for India from early March to late August, 2020

Figure 7

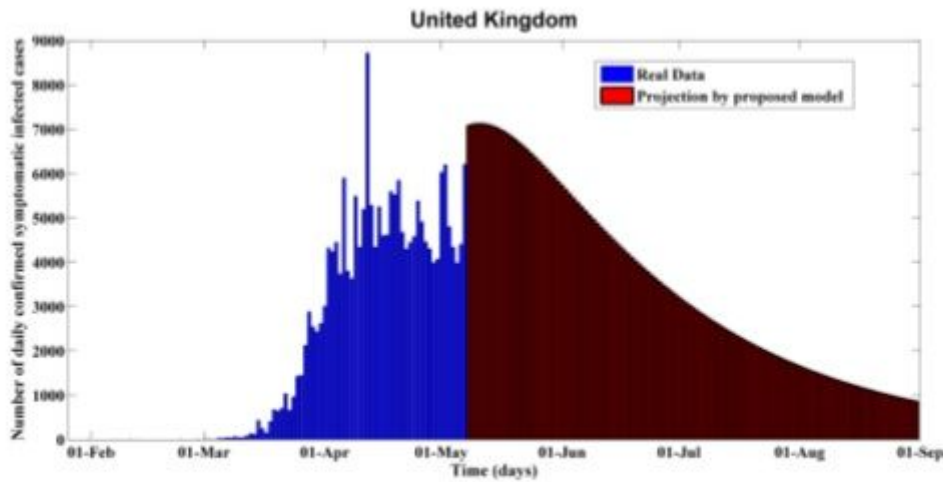
Predictions of the proposed SEIDIUQHRD model for India from late January to late August, 2020



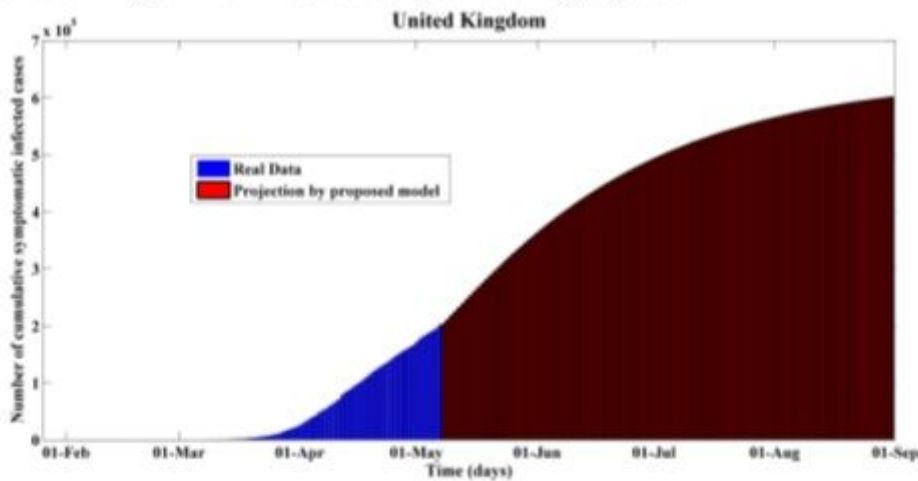
(a)

Figure 8

Fitting performance of calibrated SEIDUQHRD model for the United Kingdom from 31 January to early May, 2020



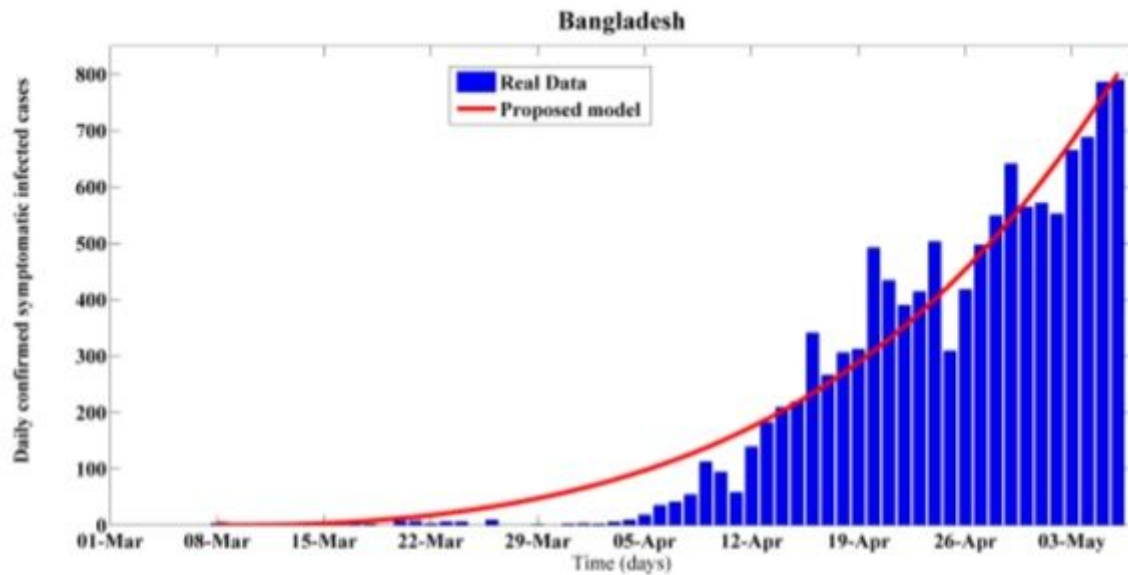
(a) The number of daily detected symptomatic infectious cases measured and projected for the United Kingdom from late January to late August, 2020



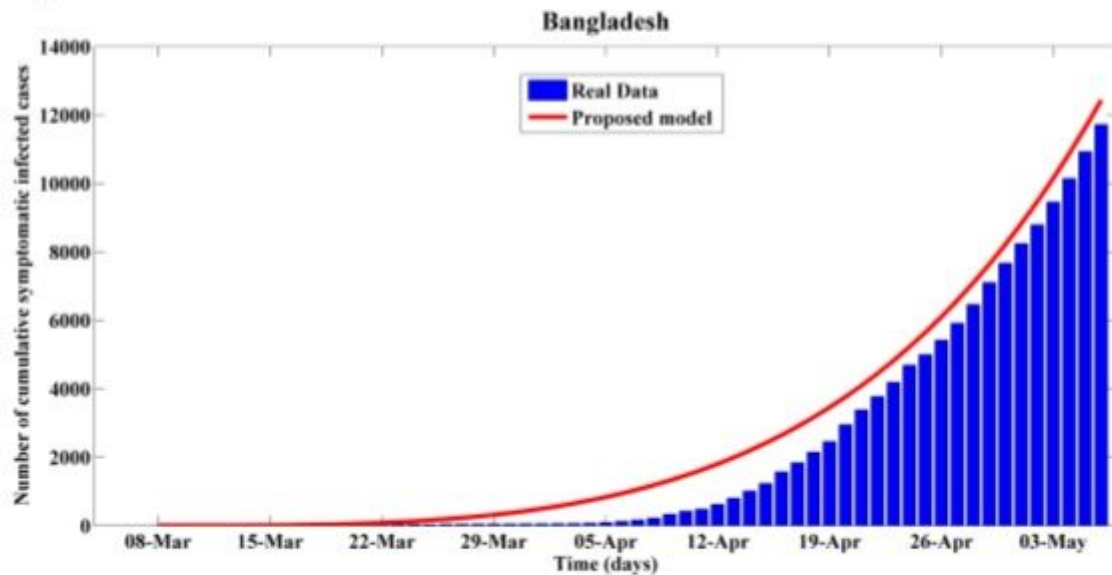
(b) The number of cumulative detected symptomatic infectious cases measured and projected for India from late January to late August, 2020

Figure 9

Predictions of the proposed SEIDUQHRD model for the United Kingdom from late January to late August, 2020



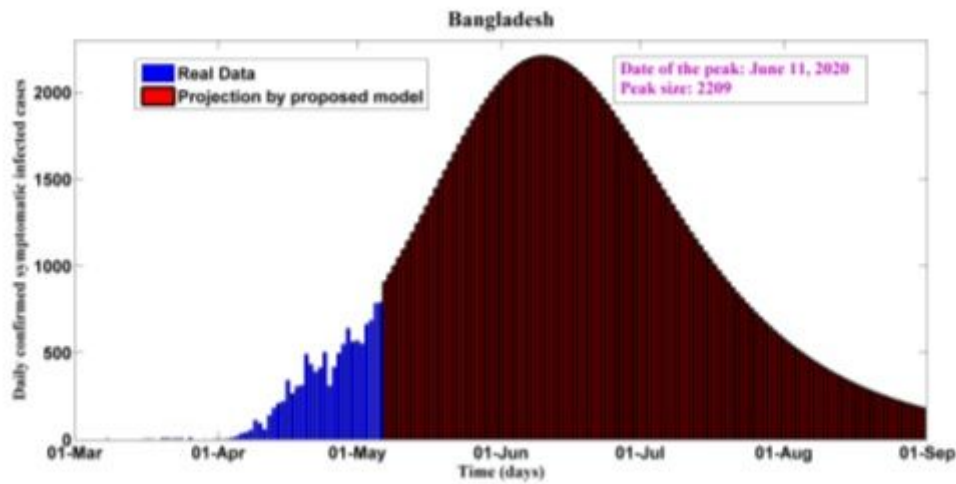
(a) The number of daily detected symptomatic infectious cases measured and fitted from early March to early May, 2020



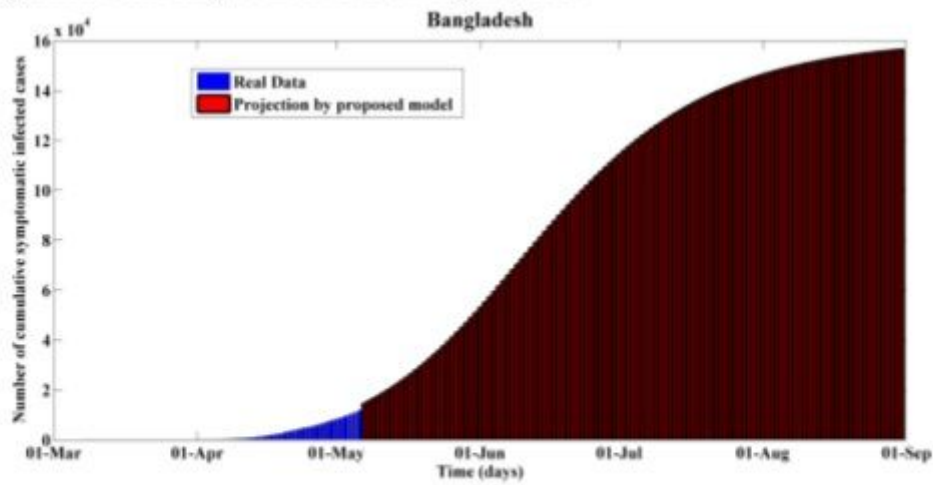
(b) The number of cumulative detected symptomatic infectious cases cases measured and fitted from early March to early May, 2020

Figure 10

Fitting performance of calibrated SEIDUQHRD model for Bangladesh from 8 March to early May, 2020



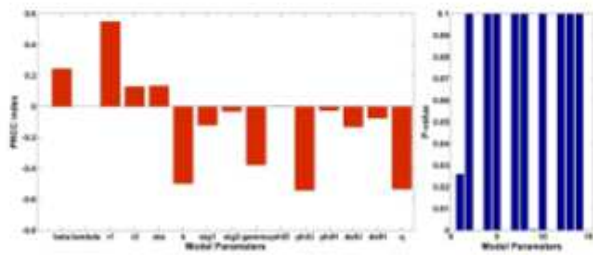
(a) The number of daily detected symptomatic infectious cases measured and projected for Bangladesh from early March to late August, 2020



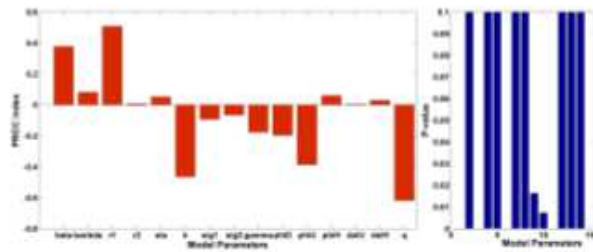
(b) The number of cumulative detected symptomatic infectious cases measured and projected for Bangladesh from early March to late August, 2020

Figure 11

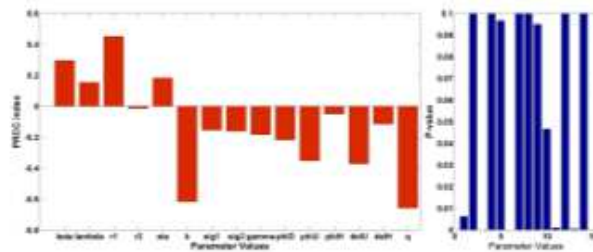
Predictions of the proposed SEIDUQHRD model for Bangladesh from early March to late August, 2020



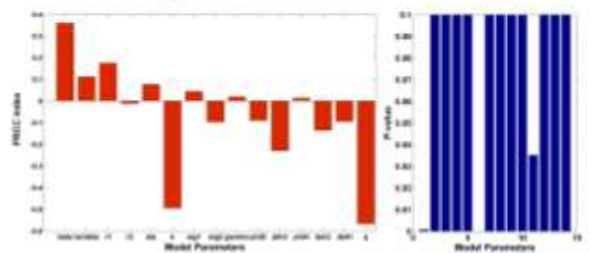
(a) Sensitivity analysis for Russia



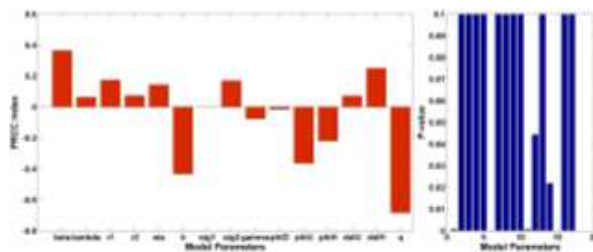
(b) Sensitivity analysis for Brazil



(c) Sensitivity analysis for India



(d) Sensitivity analysis for the UK



(e) Sensitivity analysis for Bangladesh

Figure 12

Sensitivity of the symptomatic infected cases while changing parameters in the proposed SEIDUQRHD model as indicated by the PRCC index for five different countries